CZECH TECHNICAL UNIVERSITY IN PRAGUE
FACULTY OF ELECTRICAL ENGINEERING
DEPARTMENT OF MICROELECTRONICS

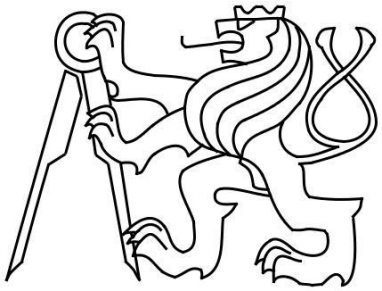

BACHELOR THESIS

DESIGN OF DATA COLLECTING UNIT FOR STABILIZING AND BALANCING PLATFORM IN PHYSIOTHERAPEUTIC APPLICATION

VIKTOR JAROLÍMEK

Supervisor: Ing. Vladimír Janíček, Ph.D.
Expert consultant: Radim Laga

Study Programme: Communication, Multimedia, Electronics
Specialization: Applied Electronics

Prague 2017

ČESKÉ VYSOKÉ UČENÍ TECHNICKÉ V PRAZE

ZADÁNÍ BAKALÁŘSKÉ PRÁCE

I. OSOBNÍ A STUDIJNÍ ÚDAJE

Příjmení: **Jarolímek** Jméno: **Viktor** Osobní číslo: **434669**

Fakulta/ústav: **Fakulta elektrotechnická**

Zadávající katedra/ústav: **Katedra mikroelektroniky**

Studijní program: **Komunikace, multimédia a elektronika**

Studijní obor: **Aplikovaná elektronika**

II. ÚDAJE K BAKALÁŘSKÉ PRÁCI

Název bakalářské práce:

Návrh jednotky sběru dat pro na stabilizační podložku ve fyzioterapeutické aplikaci

Název bakalářské práce anglicky:

Design of data collecting unit for stabilizing and balancing platform in physiotherapeutic application

Pokyny pro vypracování:

1) Prostudujte problematiku aplikací tenzometrů v medicínských aplikacích.
2) Navrhněte koncept sběrného modulu pro obsluhu tenzometrických snímačů na stabilizační podložce využívané ve fyzioterapii.
3) Požadované parametry: rychlost měření min. 200 SPS, min. rozlišení 1 g., šum max. ekv. 25 g (pp).
4) Zapojení realizujte a otestujte jeho funkčnost.

Seznam doporučené literatury:

1) Handbook of Force Transducers: Principles and Components, Dan Mihai Stefanescu, ISBN-13: 978-3642182952.
2) Implantable Electronic Medical Devices, Dennis Fitzpatrick , ISBN-13: 978-0124165564.

Jméno a pracoviště vedoucí(ho) bakalářské práce:

Ing. Vladimír Janíček Ph.D., katedra mikroelektroniky FEL

Jméno a pracoviště druhé(ho) vedoucí(ho) nebo konzultanta(ky) bakalářské práce:

Datum zadání bakalářské práce: **09.02.2017** Termín odevzdání bakalářské práce: **26.05.2017**

Platnost zadání bakalářské práce: **10.09.2018**

Podpis vedoucí(ho) práce	Podpis vedoucí(ho) ústavu/katedry	Podpis děkana(ky)

III. PŘEVZETÍ ZADÁNÍ

Student bere na vědomí, že je povinen vypracovat bakalářskou práci samostatně, bez cizí pomoci, s výjimkou poskytnutých konzultací. Seznam použité literatury, jiných pramenů a jmen konzultantů je třeba uvést v bakalářské práci.

. | Datum převzetí zadání

Podpis studenta

AUTHOR STATEMENT FOR UNDERGRADUATE THESIS

I declare that the presented work was developed independently and that I have listed all sources of information used within it in accordance with the methodical instructions for observing the ethical principles in the preparation of university thesis.

PROHLÁŠENÍ AUTORA PRÁCE

Prohlašuji, že jsem předloženou práci vypracoval samostatně, a že jsem uvedl veškeré použité informační zdroje v souladu s Metodickým pokynem o dodržování etických principů při přípravě vysokoškolských závěrečných prací.

In Prague 2017

.....

ACKNOWLEDGEMENTS

I would like to express my deepest gratitude to my expert consultant and mentor, Radim Laga, for his support and guidance throughout the whole time I worked on this project, who also allowed me to further understand my field of study. I also wish to thank Ing. Vladimír Janíček, Ph.D. for his support, encouragement and valuable advice he provided at any time I needed it.

ABSTRACT

This thesis presents a process of design, development and testing of a new data collecting unit for a stabilizing and balancing platform that is going to be used in physiotherapy. The paper describes the schematics and the process of their design, along with new changes that were made in the process, but also introduces the problems encountered during the development. There is also a significant part about various issues, for example a number of components, power dissipation within certain components and others.

Keywords: design, data collecting unit, stabilizing and balancing platform, schematics

ABSTRAKT

Tato bakalářská práce pojednává o procesu návrhu, vývoji a testování nové sběrné jednotky pro stabilizační a balanční plošinu, která bude použitá ve fyzioterapii. Práce popisuje schémata a proces jejich návrhu, spolu s popisem různých změn, které byly v průběhu vývoje provedeny, tvorbu samotného plošného spoje a s návrhem spojenou problematiku. Zároveň se zabývá i různými problémy, které bylo potřeba vyřešit, a to například: počet součástek, zahřívání určitých částí a další, tomu podobné.

Klíčová slova: návrh, sběrná jednotka, stabilizační a balanční plošina, schémata

CONTENTS

GLOSSARY

ADC – analog-to-digital converter
CLK – clock
COP – center of pressure
CS – chip select
DAC – digital-to-analog converter
ESD – electrostatic discharge
LC – load cell
LDO – low-dropout regulator
MCU – microcontroller unit
MISO – master in slave out
MOSI – master out slave in
MUX – multiplexer
Opamp – operational amplifier
PCB – printed circuit board
PE – protective earth
PSRR – power supply rejection ratio
PWM – pulse width modulation
SPS – samples per second
VAT – value-added price

1. INTRODUCTION

1.1. MOTIVATION

With this project, I have become a part of a team that has been working on a special physiotherapeutic machine for the past year and a half. There have been many different designs and the electronic insides have always had to adjust its size and shape accordingly, so they would fit along with the mechanical parts. For this reason, there have been many board designs, but as the project nears its final stage, all the parameters are being finalized. The main circuit board – called gener – was too big to be used for the marketed product, so it has been divided into several smaller boards and its functions were broadened. The process of creating one of these boards is covered in this work on the following pages. The aim is to implement the designed circuit board in a real world application for the physiotherapeutic machine that is being developed by one of the most renowned companies on the market.

1.2. ASSIGNMENT

My task was to design a data collecting unit PCB for a stabilizing and balancing platform, which is going to be used in physiotherapy. As the board is supposed to work in sort of a medical device, there are certain parameters that have to be met in order to ensure a correct functionality of the machine, because readings from this machine can determine, whether someone becomes a patient, or alternatively, how is a patient going to be treated. The board will work with an ADC and collect data from load cells (strain gauges). These data will then be transformed into weight and weight distribution across the platform (explained further in the text). And for this reason, certain criteria have to be guaranteed. First of all, there is an issue of resolution, which needs to be lower than 1 g, so the machine reacts accordingly as fast as possible when there is a real time change on the platform. Secondly a matter of noise, which will affect the overall readings. It was determined that a peak to peak noise of 25 g should not cause any problems. And last but not least, the sampling speed of the ADC, so the readings are as clear as possible but also fast enough to provide a suitable response to the input from the patient. The sampling speed was set to be 200 SPS. And for my final task, I was to test the board in real time application and determine, whether it can be used or not. These are the main goals of the assignment, but not the only ones. The rest of them, as for example certain functionalities and tests, will be mentioned and described along the way of the designing process. All of this was tasked by a Czech company – BTL – Medical Technologies and will be used in one of their products.

2. THEORETICAL INTRODUCTION

2.1. BTL - MEDICAL TECHNOLOGIES

BTL is a Czech company, which specializes in three branches – physiotherapy, cardiology and esthetic medicine. BTL is one of the biggest developers in applied medical appliances all around the globe and is well renowned for its products even across the ocean in the USA. Highly skilled teams of hardware and software developers work on creating new ways of helping people through high tech medical machines. With subsidiaries in 54 countries in the world, BTL comes close to being the biggest company in its field. The company focuses on real time applications instead of aiming for new discoveries in biomedicine. That allows them to develop their products faster and with more reliable outcomes, because all of their base concepts have already been proven and certified.

2.2. STABILIZING AND BALANCING PLATFORM

Main purpose of the machine in development is a use in physiotherapy. It will allow for diagnostics, rehabilitation and working out of the weakened muscles. The platform is underlaid with four load cells that can withstand up to 500kg of immediate weight (safeguard against jumps and unexpected loads) and can accurately measure the weight of the patient in the matter of tens of grams. Two load cells are also going to be placed in the handles so they can monitor whether the patient pulls or pushes while balancing on the platform. Everything is going to be controlled via special screen with graphic interface that is going to display control settings, navigation menu, graphs and other functionalities. For emergency situation, there is a big red button that immediately stops the whole machine, so there is no threat to the patient even during unexpected accidents (e.g. sudden dizziness, nausea, loss of balance, ...).

Furthermore, the platform offers 3 different modes of operation.

1. Measuring of COP – diagnostics
2. Working out – you either follow the instructions on the screen or have to counter balance the motions of the platform
3. Casual – games and other features

Ad 1

The platform is able to measure the distribution of weight between the feet. This can reveal certain disbalances in patient's stance, which can alarm the professional, operating the machine, to further investigate the cause of this uneven distribution of weight, such as different length of legs, scoliosis, muscle disbalances and so on.

Ad 2

Two special possibilities are available in this mode. The first one guides the patient through the workout routine with instructions on the screen and he/she has to move his/her weight in a specific direction to move the platform. The second one moves the platform on itself and the patient has to balance his/her body in order not to fall off. That leads to strengthening of various muscle groups in one's body, improves balance, posture and muscle reflexes.

Ad 3

This mode contains features like games. The patient can move the platform with his/her weight to move a board on the screen and bounce the ball off of it. Or he/she can distribute the force he/she applies on the platform in a similar way as one does when he's/she's skiing and a skier on the screen will turn and go around obstacles. This way the patient can perceive the experience as more interesting while improving certain aspects of his motor skills.

2.3. PARAMETERS

Parameters given in the task have to be calculated somehow. While the sampling speed is going to be determined by the architecture of the board, filters and other methods, the resolution and peak to peak noise can be calculated. Or to be more specific, I can calculate the maximal values of other parameters, which need to be reached in order to meet the parameters given by the assignment. The Table 1 below shows the parameters. The output sensitivity and FS is given by the load cell, excitation voltage was experimentally set, because with this value, the LC output is significant enough for us to read and the rest is self explanatory. However, not the way I calculated the resolution and peak to peak noise, so I am going to make that a little clearer in equations (1), (2), (3).

$$Resolution\ \left[\frac{g}{LSB}\right] = \frac{Basic\ resolution}{LC\ output} = \frac{\frac{Voltage\ range}{Smallest\ increment}}{LC\ ouput\ for\ 1g} =$$

$$= \frac{\frac{Vref\ (ADC)}{ADC\ resolution\ (bits)}}{LC\ output\ for\ 1g\ \cdot gain} = \frac{\frac{2.5\ V}{2^{24}}}{6.4 \cdot\ 10^{-6}\ V} = 0{,}023\,\frac{g}{LSB} \qquad (1)$$

Most of the values here are constants, so the only thing I could change would be the voltage reference. This one is set by the ADC I am using and therefore is given and unchangeable (in case of a change, the resolution would a little lower and the noise in the ADC would have had to be lower too, as the noise in grams is directly dependant).

$$Noise\ [g] = Resolution\ [g] \cdot ADC\ noise\ (raw\ value\ [-]) \qquad (2)$$

$$PeakToPeak\ Noise\ [g] = Noise\ [g] \cdot 2 \qquad (3)$$

Equation (2) could actually be calculated for the ADC noise value, because the noise value in grams is preset by the assignment (<25 g). But from the equation and Table 1 below is clearly visible the maximal value of the ADC noise that is tolerable. The peak-to-peak value (3) is simply just a doubled (2), because it can go both ways from the relative zero value.

Table 1: Table for calculating resolution and noise parameters (FS = maximal load)

Load Cell		
Output sensitivity FS	2	mv/V
FS	200	kg
Excitation voltage	5	V
ADC bits	24	
ADC VREF	2.5	V
GAIN (ADC)	128	
Noise ADC (raw value)	530	
LC output FS	10	mV
(LC output FS)*GAIN	1280	mV
LC output 1g	0.05	uV
(LC output 1g)*GAIN	6.4	uV
Resolution	**0.023**	**g/LSB**
Noise	**12.340**	**g**
Peak-to-peak noise	**24.680**	**g**

2.4. MARKET RESEARCH

The whole board needs to be designed according to specific instructions so it can meet the requirements that are put on it by the final product. That doesn't allow me use a circuit board already in existence. But on the few following lines, I would like to summarize, why it is also impossible to create a modular board from smaller board designs on the market.

The most important part of the LC Core board is the part which processes the signals from the strain gauges. Firstly, it is undoubtedly more profitable to use a load cell that already contains a bridge circuit, which allows for auto-compensation. The load cell I used was selected to fit the parameters given by the machine specifications. Regular weights available on the market cannot hope to reach the sensitivity that is needed for correct and precise measurements to determine the weigh distribution of the body. Problem with separate load cell amplifiers and circuits at lower prices is their weight range, which is lower than what is needed for our platform. That is up to 200 kg of raw weight with the possibility of handling and processing higher values in case of sudden tremors and shocks. In the table below, I have listed a few evaluation boards I have found in online stores (Farnell, Mouser, Aliexpress) and compared them to the parameters given by the assignment.

Table 2: Comparison of various boards available on the market

	SPS	Nr of LCs	Price [Cr]	Bits	PWR supply
Desired	200	4	lower than separate parts	24	5V
AFE4300EVM-PDK (TI)	up to 860	4	5234,3	24	9V
DIYmall HX711 (arduino)	10/80	1	25	24	up to 5.5V
EVAL-CN0216-SDPZ (AD)	120	1	1730	24	6V
ADS1131REF (TI)	10/80	1	1384	18	up to 5.3V

Even though the first board meets the parameters needed, the price exceeds the expenses that would be required for me to build the board from scratch. Moreover the board should be multifunctional while taking up as little space as possible due to the space restrictions.

As mentioned above, this table covers only one of the modules that would be required for the whole component. Regulation of diodes could be done via shift registers, multiplexers or LED matrixes, but these are mostly done on a single board or would require extensive wiring, in order to execute the proposed design. For this reason it is faster and more efficient to design our own model.

Another important aspect of the boards is its size, which need to fit the machine space that was left by other components. Creating a modular board would create more difficulties considering the connective wires, space management, parameters selection and would make the company dependant on the board supplier in the future.

2.5. SOFTWARE

2.5.1. ALTIUM DESIGNER

As the main designing software, Altium designer [1], version 17.0.1 was chosen. It offers wide variety of customization on both schematic as well as PCB designing side. It also allows usage of special company libraries that include stored and tested components. That sped up the schematic concept development, because it minimized the number of changes that would have been caused by inaccessible fitments or improper values.

2.5.2. LTSPICE IV

Simulations were done mostly in LTspice IV [2]. (The newer version, LTspice XVII, doesn't offer anything that would improve the results of my simulations so there was no reason to choose this one over the older version, that's always been used in BTL). LTspice offers its own library of components, with input parameters, that make the simulations faster and easier. It is also possible to input customized/specific components to make the simulation more accurate in cases, where I would have to choose just a similar part instead of the correct one. LTspice allows for voltage, amperage, thermal, time and other measurements, which are crucial to ensure the correct functionality of the design under different circumstances and excitation values.

2.5.3. STM STUDIO

Special graphic studio invented by microchip [3]. Using STM Programmer to connect the board to the computer, it allowed me to watch the ADC response in real time along with the changes while the load cell is being stressed. With a special variable in the software, added by the team's software developer, I was able to check the ADC output. A raw value, coming out from the ADC, displayed the noise that was created either in the ADC itself or got accumulated on the single along the way to the ADC. This was crucial in determining the

right setup for the ADC filters and for checking, whether the signal from the load cells is even viable for further processing or if there are changes that have to be done to the hardware design to clear up the signal.

2.5.4. ST-LINK

ST-Link [4] enables connection between the ST-link programmer on the board and the computer. This gave me an insight into to communication between the PCB and the microcontroller using I2C (MISO, MOSI, CS, CLK) communication. That greatly helped to determine the origin of problems, when there were no data from the ADC outputs.

2.6. HARDWARE

Most of the hardware parts were already chosen in the previous versions of the PCB board. For that reason, my ability to select them was restricted to using parts that are available in the company storage supplies. All the parts, that were available had been tested before and are proved to be working in all previous designs and in other machines that had been developed by BTL engineers. The selection process for every new component has to undergo a series of tests and authorizations, everything in order to achieve the highest efficiency. There are different criteria to be met. Even though the price of the part is important, it is not the main factor as one might think. Several of the most important ones are customer support, available software for development and peripheries. Considering every part is to be used in a commercial machine, it always has to be ensured, that the parts are easily programmable with high quality software environment. Furthermore, it is not unusual that certain parts do not always work according to the manual/datasheet or do not always react the way we would expect them to in different settings. Customer support is therefore another important aspect. One more condition worth mentioning is that it is not possible to institute a new part for just one project. There should always be another project that would or could use the part now or in the future. For the reasons stated above, my designs build on the parts that had already been registered to our database. It also allows for every part in every design to be right at hand when one needs it, which speeds up the development process.

2.6.1. LOAD CELLS

L6E Zemic load cell [5], with weight range up to 200kg. Tested to withstand up to 500 kg of raw force, caused by sudden shocks and jumps. L6E contains a full bridge wiring, which leads to differential output and temperature compensation. A 4 conductor cable with shielding ensures as low interference during transmissions as possible.

In our case, we are going to use 4 load cells, placed in specific positions around the platform, which will allow for precise measurements and sufficient maximal possible weight. In comparison to a standard scale we have at home, our topology allows us to measure the distribution of weight across the platform. A scale would do with a single load cell that only measures the weight of the person and nothing more is needed for its

functionality, which is often the reason why the result is always a little different from the previous one. While our four load cells, located in the right places, can distinct the stress between left and right foot as well as between the overbalance on the patient's toes or on his/her heels.

2.6.2. ADC

24-bit, low noise, low power, ΔΣ ADC. AD7124-8 from Analog Devices [6] was chosen. SPI compatibility also fits our needs. There are 8 differential channels, which would suffice for connecting all load cells to one ADC. But be it the case, that more ADCs would have to be used for the final board design, there would be no reason to switch to a ADC with lower number of channels, because the price is actually two dollars per piece higher and the chips remains completely the same, only with the channel pins cut off. AD7124-8 also contains many different settings, allowing for different sampling speeds, from 1.17SPS up to 19200SPS. These also determine the background noise behind the transmitted data, so the software, controlling the ADC, has to be set up carefully. Furthermore, there are many different filters available. It is possible to set a 50Hz/60Hz rejection, sinc filters and various sampling modes. However, these have hard set sampling speeds that cannot be changed or combined. Another upside is its own ESD protection, which will save some space on the final design.

The number of ADCs, its filters and settings needed to fulfill the given measuring parameters had to be determined and will be described further in the text.

2.6.3. ACCELEROMETER

To better keep the platform's position in check in order to determine the tilt of the balancing board, an accelerometer was added. BNO055 [7] offers 3 sensors in one device, a gyroscope, a geomagnetic sensor and a triaxial accelerometer. The last one is the function we are going to use in our machine. With 1,7V-3,6V voltage range, it perfectly fits in with the rest of the components, so there is no need to add another power branch to the design. 1° change is determined by 16LSB. The reason, why the accelerometer can be crucial for our machine is that tilting the platform by even a single degree can significantly influence the weight distribution of the patient. Also during the workout mode, improper platform position can force certain muscles to stay active the whole time and therefore make the preprogrammed routines ineffective or even harmful. Tilting the platform more than it is allowed could also cause loss of balance of the trainee, which could lead to injuries. As for the risks on the mechanical side, the platform by itself can move up to ±15° and if the programme assumes an incorrect tilt, it could try and force the board to move over the limit and cause permanent damage on the system.

Processing the signal and determining the axis position is part of the software solution and therefore above the contents of this work.

2.6.4. MCU

A 64 pin microcontroller unit STM32F405RGT6, LQPF-64 [8] was used as the best suited choice for our board. Its size and number of pins with various peripheries fit my PCB without a hitch. There are several ports supporting USART, I2C and SPI. Many different TIM general timers with variety of special functions, which can be used for PWM and other types of control. Internal ADCs and DACs both have low sensitivity for certain uses but still can provide a valuable help in specific designs. Therewithal every port can be used as an "EVENTOUT" event, which allows for a specific function to be set by the user via software programming.

2.6.5. LT, LM

LT6221 [9] and LM1117 [10] were chosen to help us in creation of the circuit design.

LT6221 [9] operational amplifier can be used in various integrations. Everything depends on the parameters that would be required. Even though LT can be used as a substitution for a comparator, integrator and so on, its capabilities might not be sufficient for certain applications. The main purpose of LT6221 [9] in this board is to amplify the power for load cell units.

LM1117 [10] dropout linear regulator was utilized to downregulate the input voltage coming to the PCB. Even though its dependencies on different aspects (current, capacitance) would have to be tested in order to determine whether a more sophisticated stabilization is on order or not, this component seemed to be ideal for my application.

2.6.6. BSS, NTD

There are few transistors used in my design, chosen in order to comply with specific threshold voltage, speed and other parameters. Most of them are power transistors, used to control the LED architecture, while some serve as a part of current limitation process. The most used ones are BSS84 (PMOS) [11] and NTD5865 (NMOS) [12]. BSS138s (NMOS) [13] were used in some of the initial designs but were scratched out later on.

3. DESIGN AND TESTING

3.1. ADC

One of the main issues that had to be resolved was the number of ADCs, which would be needed for my design to fulfill the desired parameters of the measuring unit. Every converter can be set via software to use a preset filter, which influences speed of sampling as well as the quality of the output data (the amount of noise by which will the result be distorted). The process of determining consisted of using the binary file, written by our software engineer, manually changing the ADC filters and consecutively measuring the output in STM Studio and analyzing the results. All of that was done using the previous version of the board. Using the Eclipse [14] programming environment with STM plugin for MCU programming [15] I changed the values and variables of various filters through adjustments of their representing bits, taken from the datasheet [8]. The graphical representation of the data coming out of the ADC was executed using the STM Studio, which allowed me to watch a specific variable that stored the immediate raw value from the converter. Our ADC is a 24-bit Σ-Δ converter, therefore the highest possible raw value is 2^{24} and for our purposes, so the system can also detect a force lifting the platform, we moved the relative zero value to the middle of the maximal range, which means that in static state, the value coming out of the ADC, a relative zero, is 2^{23} and the oscillation around this value in an unencumbered state is pure noise. Along with the graphical representation, it was possible to get a real value of SPS in a single time cycle. Using stop points and reading the stored sampling speed value in a certain number of cycles, creating an average figure, enabled me to compare the real obtained results with the numbers stated in the ADC datasheet [6].

However before determining, which filter would turn out to be the best possible solution, I had to deal with the distortions of the signal. It seemed that the signal is burdened by a specific source of noise, which was nearing the state, where the useful signal would be drowned in noise. If the graphical representation of the signal was launched for a longer period of time, it was possible to recognize a sinus-like envelope around the signal. There were several causes that came to mind. Problem within the cable, with which the signal was led, the design of the board/circuitry or the surrounding noise in the network. Considering the overall shape of the signal, which reminded a sinusoid, it seemed possible that there is somehow a way that the power signal coming from the socket is affecting the useful signal we are processing. To avoid changes in the power branch of the board, which might have had a clear result, we decided to try a simpler approach. We connected the ground part of the board to the PE peg in the socket. That significantly lowered the variance of the signal. It did not erase it completely, but the sinus-shaped enveloped disappeared and the resulting signal was a lot clearer. The Figures 1 and 2 below show a clear distinction between the signal before and after connecting the PE peg (in the terms of raw value, the difference is somewhere around 800 units):

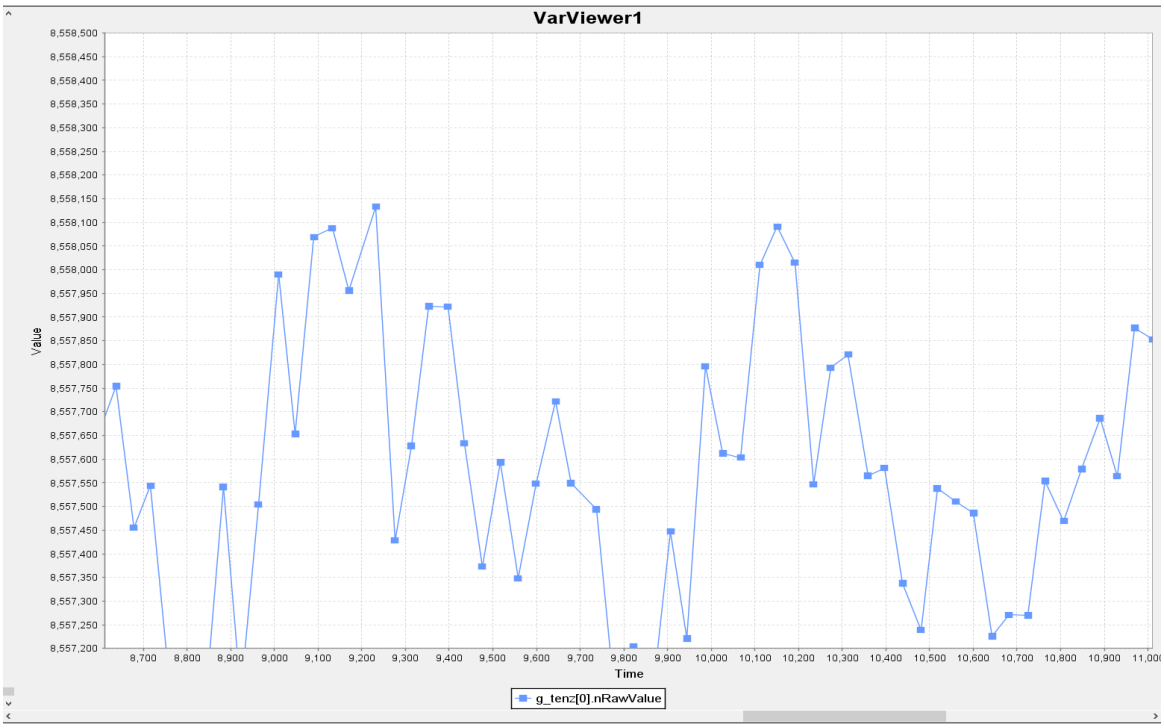

Figure 1: Exemplary course of raw ADC output (No PE - 20ZL filter applied; *axis X = time [s], axis Y = raw value [-]*)

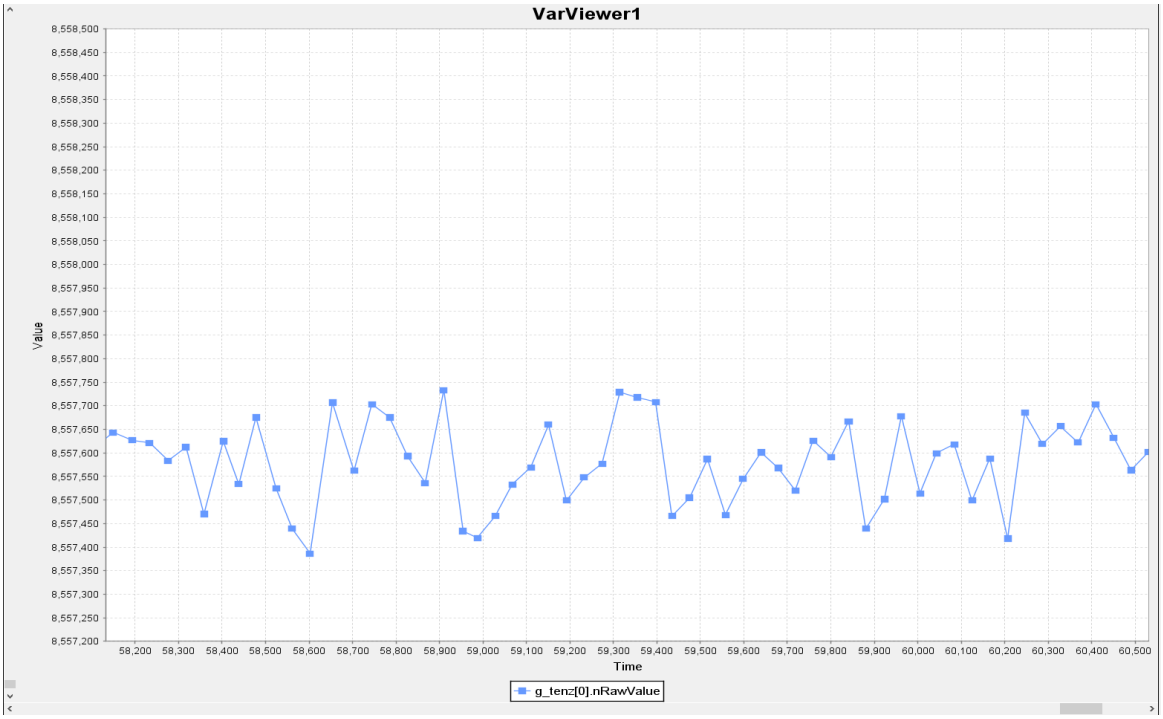

Figure 2: Exemplary course of raw ADC output (PE peg + 20ZL filter applied; *axis X = time [s], axis Y = raw value [-]*)

Even though the biggest contribution to the noise level was caused by the power network, it was still unclear, whether the rest is caused by the wrong circuit design, the cables the inner noise caused by the ADC or something else entirely. So before blaming it on the incorrect filter setting, I had to determine that it isn't cause by something that could be eliminated on the hardware side. Our main culprit was the ADC and for this reason, we

decided to go around the other parts that could be causing the inaccuracies within the signal. I unplugged the load cell and short-circuited the connector inputs. With that, the only thing, which should be visible on the output would ideally be the set value – 2^{23} (8 388 608). And the output was measured via the STM Studio software by watching the corresponding variable. (So there were no more circuitry or external conductors, which could distort the signal.) The Figure 3 shows the measured trait. With this, I managed to confirm that the rest of the noise is mostly caused by the ADC and therefore can be reduced by setting the right filter.

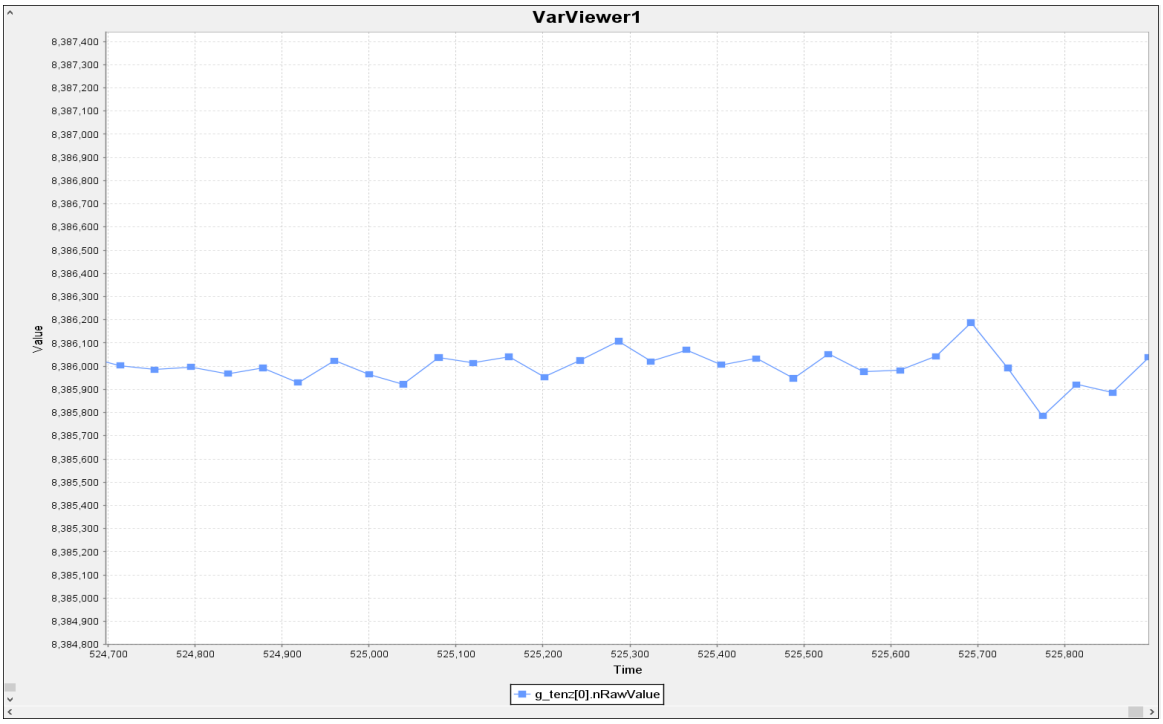

Figure 3: Short-circuited LC input - pure noise of the ADC (Axis X = time [s], axis Y = raw value [-])

The possibility to use one ADC for all four load cells was rejected right away as it would lead to a signal that would be drowned in too much noise, which would result in lowered sensitivity. The issue then remained whether I would need on ADC for every load cell to meet the required parameters or if I could use two ADCs for all four load cells.

As my desired sampling speed was 200 SPS, I managed to find a filter that would allow me to use two ADCs, each handling two load cells, which still has an acceptable noise ratio added to the strain gauge signal. To give a better insight into the STM Studio measurements, please see other Figures 1 and 2 above this paragraph. All of my findings can be seen in the appendix [Appendix C], where every measured SPS value is made as an average from multiple measurements. As a result, the sinc3 filter was chosen as the best suited one for our platform.

Connected to the issue above, there was a question of the gain in the ADC itself. There are 8 options available, ranging from 1 to 128, all of them of course influence the output clarity. The higher the gain, the more noise in the final signal. In the very beginning, when the AD7124-8 was implemented in the project, it was decided that the 128 gain is going to be used. For that reason, it had to be checked that the LC output voltage is significant enough

that it would be recognizable in the surrounding noise from the ADC. As mentioned before, we were working with the raw value from the ADC that is later calculated into t he final weight. The maximal range of the ADC is 2^{24} (16777216) units (raw value), moved to the middle value (2^{23} = 8388608). Therefore the changes that come with the new distribution of weight across the platform had to be significant enough, so the board would be able to process them correctly (meaning that had the change in the raw value from zero to a hundred kilograms was for example just about 10 000 of raw value, the difference for smaller changes would be almost unnoticeable and therefore the machine would not suffice for weight distribution measurements). Precise weights were available in the office (100g-5kg). A jump increment of the weight was introduced to the load cell system, to see the response and the change in the raw value.

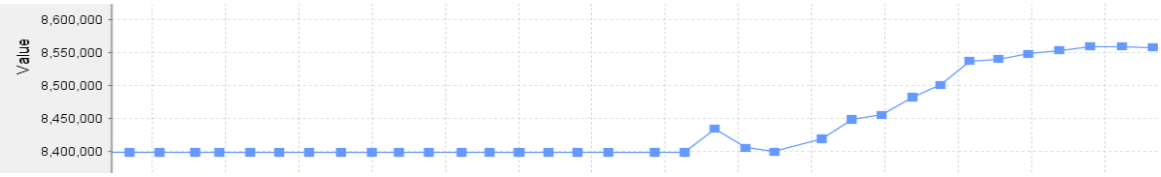

Figure 4: 0 kg to 10 kg load jump change over 0.5 s. (Axis X = time [s]; axis Y = raw value [-])

The whole graph can be seen in the appendix [Appendix D-D1], but the change is roughly 160 000 of raw value for a 10kg weight (16 000 for a single kilogram). This concludes a high enough resolution/transition between the value in the ADC and the output result. Had the jump in the raw value been too low, it would be hard to recognize smaller changes in the weight distribution across the platform and either the gain would have to be externally increased or a higher power supply voltage for the load cells would have to be implemented.

Gain parameter was mentioned in the previous paragraph and in order to support my claim that the ADC is working with a constant gain of 128, I decided to do some extra measurements to check the actual amplifying value. We designed a circuit with the ADC but with some extra components. To make the signal detectable by our multimeter, I boosted the signal 4 times. The gain is a little bit different from 512 (4 x 128) due to variations in the value of the components, but in this case, we do not mind, because the main aim is to see that the gain remains the same while increasing the load on the load cell. Working with different weights, I took a value in front of the ADC and a value coming out of it. After that the amplifying parameter could be calculated and can be seen in the following Table 3. There is always something mixed in with the signal due to the surrounding machines and particles in the air. Because the interference is very low, it is only detectable in the weakest signals as can be seen for the 10 g load. The rest of the gain is fairly constant and therefore supports our expectations.

Table 3: Table of gain measurements

WEIGHT (g)	BEFORE [V]	AFTER [V]	GAIN [-]
10	5,00E-07	3,20E-04	640
50	2,50E-06	1,30E-03	520
100	5,00E-06	2,70E-03	540
150	7,50E-06	4,07E-03	543
250	1,25E-05	6,70E-03	536
300	1,52E-05	8,05E-03	530
500	2,54E-05	1,34E-02	528
600	3,06E-05	1,61E-02	526
750	3,81E-05	2,01E-02	528
850	4,32E-05	2,28E-02	527
1000	5,10E-05	2,68E-02	525
2000	1,00E-04	5,35E-02	535
3000	1,53E-04	8,03E-02	526
5000	2,54E-04	1,34E-01	527
6000	3,05E-04	1,60E-01	526
7000	3,55E-04	1,87E-01	526
8000	4,06E-04	2,14E-01	526
10 000	5,08E-04	2,67E-01	526
80 000	4,43E-03	2,33E+00	527

Another test that had to be carried out was temperature dependency of the converter. Considering our board and load cells are going to be located right next to the motors that move the whole platform, a higher working temperature is expected. Thanks to the structure of the load cell, which contains a series of strain gauges wired to a Wheatston bridge and their temperature compensation is therefore ensured, yet while the ADC operating temperature is listed in the datasheet it still had to be tested, so we could safely claim that the measurements are still accurate even during machine's prolonged running state. Using a special heating chamber, we tested the board and its temperature stability. The whole board was put into the chamber while the unweighted load cells were outside and the temperature was steadily raised from 10 to 70 °C. The measurements were taken every 10 degrees. To receive a broader spectrum of tested elements we tested an output for every one of the four load cells connected and two different ADC running simultaneously. Appendix [Appendix E] displays the stability of the ADC, which shows that it is perfectly suited for our use. The biggest difference there is roughly 1200 units of raw value, which is, according to the Figure 4 above equal to less than a 100 g.

As the ADC – MCU communication is mediated with SPI, it was crucial to create a simple way to check the communication status at any point (to affirm that both components are responding well to the controlling software). For this purpose, five test points were included in the design, one for every part of the communication process. MOSI, MISO, CLK and two chip selects, one for every ADC. I myself used the test points on the previous version of the board. I used an analyzer and the ST-Link programme [4] to watch the SPI communication. Firstly it was needed to connect the right analyzer cables to the right parts on the board. Thanks to the color distinguished cables of the analyzer, it was easier to repeat the process. Green for CLK, yellow for MOSI, red for MISO and orange for chip select. From that we were

able to see whether it is gathering data or if the chip selects are changing accordingly to the software setup. With this, we were always able to closer determine the cause of miscellaneous problems.

3.2. SCHEMATICS

3.2.1. MAIN + MCU

Most of the MCU design depended on the pin mapping, which is going to be described a little further in the text. But apart from the standard power supply wiring and EEPROM memory, there are couple of added components in the schematic viz. [Appendix A6]. First of all a connector for a programming tool. To avoid unnecessary high profile connectors, we chose an old school built in connector, TC2030 [16]. Also an external reset button to simplify it for the mechanics and other engineers, who are either working on the development or will work with the platform in the future.

First couple of pins are ADC input pins and were reserved for heat sensors, or to be more precise, for connectors for the heat sensors. These are there to monitor various parts and allow for adjustments in measurements or safety measures. There is a simple RC circuit to clear the outcoming signal as can seen in Picture 1.

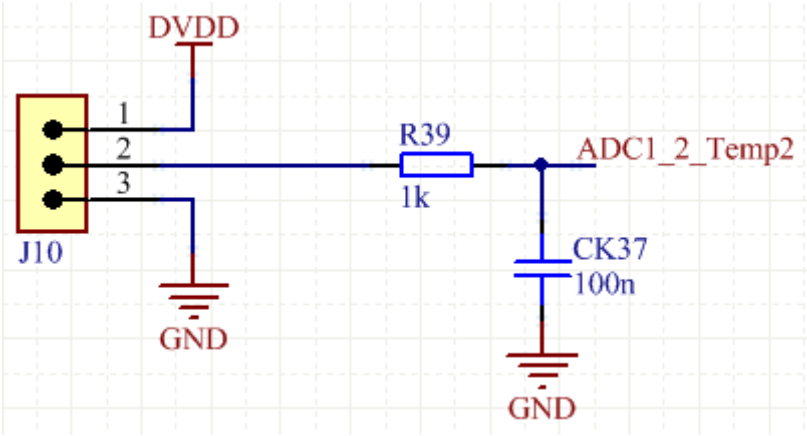

Picture 1: Heat sensor wiring

Another added part is an external 8 MHz oscillation crystal. As seen on the picture below Picture 2 there are two capacitors connected to the crystal. These ensure the correct impedance, respectively reactance, which is needed for the correct oscillation frequency of the crystal [17]. The datasheet [18] states the load capacitance to be 18 pF. As that is not a standard value, I had to pick a different one from the company's storage. 22 pF should work without any problems.

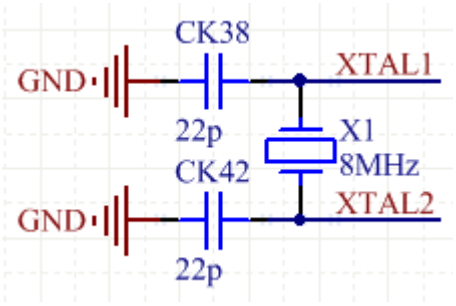

Picture 2: External oscillation crystal wiring

Moreover, the MCU handles the whole board. Even though the firmware is handled by our software engineer, it was up to me to map the pins and pass on the information. As mentioned before, from the LQFP64 denotation we can deduce that there 64 pins available. Out of these 64, roughly three quarters are actually at my disposal, the rest of them serve specific purposes (e.g. boot, resets, power, ...). In my case, and for my final assignment, I needed pins for communication, LED (MUX + control), oscillation crystal and finally for heat sensors. Working with the STM datasheet [8], I had to find pins with the capabilities I needed. Not all functions are available for every pin so I had to fit all the pins accordingly. The following Table 4 shows my work:

Table 4: MCU pin mapping

LQFP64				
Purpose	Part	Pin name	Pin nr.	Desired func.
LED	LED1	PC0	8	EVENTOUT
	LED2	PC1	9	EVENTOUT
	LED3	PC2	10	EVENTOUT
	LED4	PC3	11	EVENTOUT
	LED5	PC4	24	EVENTOUT
	LED6	PC5	25	EVENTOUT
SPI	MISO	PB14	35	SPI2_MISO
	MOSI	PB15	36	SPI2_MOSI
	SCLK	PB13	34	SPI2_SCK
PWM	PWM1	PC6	37	TIM8_CH1
	PWM2	PC7	38	TIM8_CH2
	PWM3	PC8	39	TIM8_CH3
	PWM4	PC9	40	TIM8_CH4
CAN	RX	PA11	44	CAN1_RX
	TX	PA12	45	CAN1_TX
I2C	SCL	PB10	29	I2C2_SCL
	SDA	PB11	30	I2C2_SDA
Heat sensors	ADC1_1	PA1	15	ADC123_IN1
	ADC1_2	PA2	16	ADC123_IN2
	ADC1_3	PA3	17	ADC123_IN3
	ADC1_4	PA4	20	ADC12_IN4
	ADC_Uexc	PA0	14	ADC123_IN0
Chip_Select	CS_AD2	PB6	58	EVENTOUT
	CS_AD1	PB7	59	EVENTOUT
ACC_rst	RESET	PB9	62	EVENTOUT
ACC_int	INT	PB8	61	EVENTOUT
ST_Link	SWDIO	PA13	46	JTMS-SWDIO
	SWCLK	PA14	49	JTCK-SWCLK
	SWO	PB3	55	TRACESWO
Blinking_LED	LED	PB5	57	EVENTOUT
Core/Handle select	NJTRST	PB4	56	NJTRST
OSC	XTAL1	PH0	5	OSC_IN
	XTAL2	PH1	6	OSC_OUT

3.2.2. *LOAD CELLS*

Most of the load cell circuit consists of the ESD protection, which is shown on Picture 3 below this parahraph. Load cell itself is plugged via a connector, consisting of a power supply pin, three ground pins and two pins, which are used for differential outputs. Considering that the ESD protection is taking up most of this design, I would like to analyze it a little bit closer. The first capacitor is there to handle the initial load from the ESD charge

(consisting of a small current, hence a low energy worth, but a high voltage). The most important aspect here is for the capacitor to be of greater value than the one, which is used by the ESD gun. After that a transil (transient-voltage-suppressing) diode, capable of handling high voltage and amperage peaks, depresses the voltage to mere 5V. Then there is a resistor, limiting the current going to the Shottky diodes. And along with the capacitor, creates and RC filter of the output signal. The order of the components is crucial. Even though a transil can withstand high voltage peaks, the ESD charge is too high for the transil to handle, so without the front-end capacitor, it would burn out.

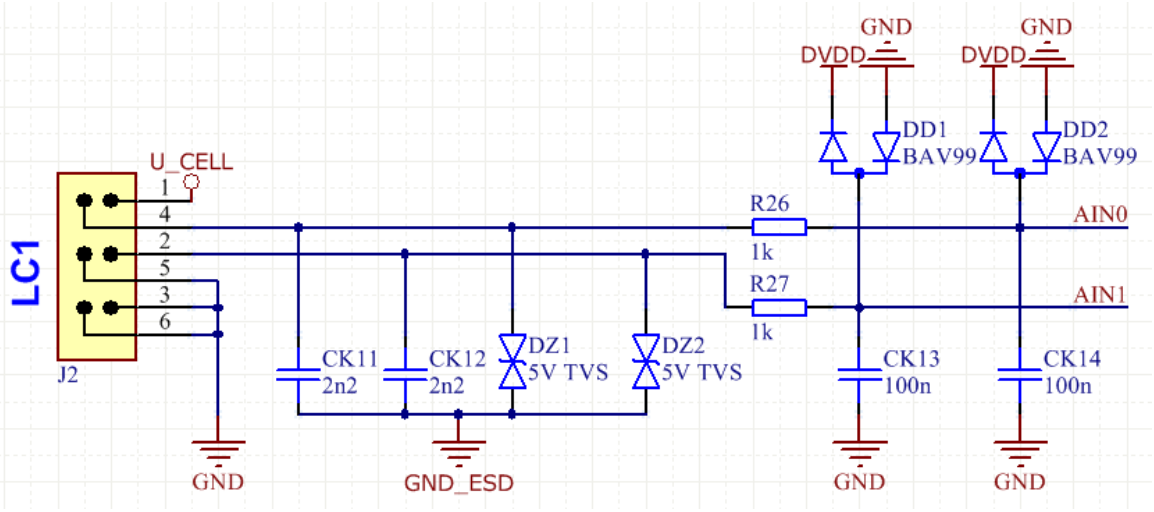

Picture 3: Load cell wiring with added ESD protection

A specific power supply circuit had to be made in order to ensure stability in the output signal. Using and ADC reference, which was amplified via LT6221 [9] opamp, I managed to assure that whenever a power supply jitters, the signal, that is being processed in the ADC remains the same, because the feed to the LCs and therefore the maximal output voltage is being referenced to a voltage, which jitters by the same amount. The whole circuit is described in more detail in the 3.2.5 Power supply chapter.

3.2.3. ACCELEROMETER

As a later feature to the board, it was decided to include an accelerometer. Its purpose is to allow easier tilt management and BNO055 [7] offers a triaxial 14-bit measurements. The wiring depends on the chosen way of communication. BNO supports I2C, UART and HID-I2C connections. Considering that the chosen MCU supports multiple I2C connections, I determined it to be the simplest and most effective. Datasheet [7] describes the correct integration which can be followed step by step to ensure the proper wiring and is depicted on Picture 4. The chosen accelerometer also supports 1.7V-3.6V feed that is why it is being powered by the DVDD node, which, as displayed in the 3.2.5., has a value of 3.25V thus sufficient enough. ACC_INT and ACC_RST are connected, along with I2C pins, to the MCU and are controlled via its software in order to start the component, reset it or gather and process the data.

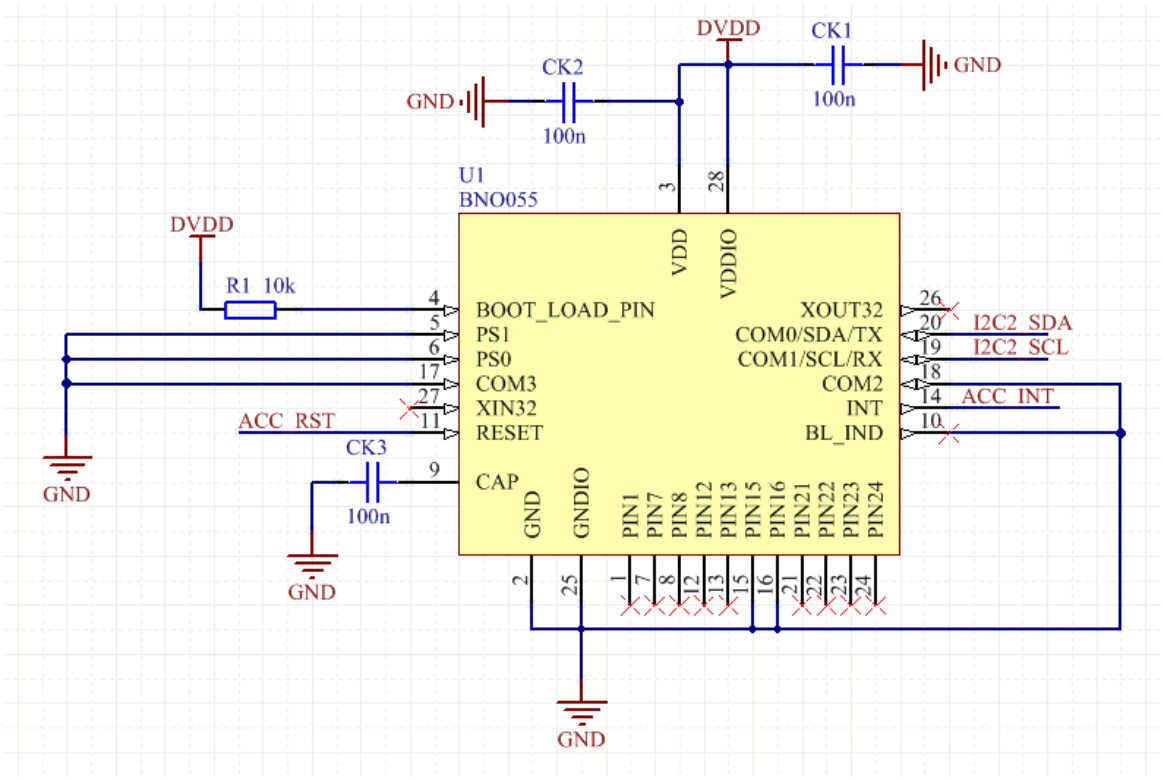

Picture 4: Accelerometer wiring

3.2.4. LED

Another late on addition were diodes, that are going to be placed around the platform to signal the patient where to transfer his weight. Over the time I have worked on the design, there had been many versions of how the diode part of the board would look like. At first, there were only supposed to be eight diodes spread across the platform in a form of a multi-color LED band plugged in via connectors. The first part of the MCU is used as MUX, it sends a signal that opens the transistors, which then in return power the LED band and keeps the power input stable. The color and the brightness of the LED bands are determined by three PWM channels from different MCU pins that allow PWM control. The combination of different PWM signals chooses the color. That would allow the programme running on the balancing machine to show the patient not only where to transfer his center of stability but also might indicate on where to channel the weight next. Picture 5 below depicts the MUX part of the diode schematics. The resistor (R24) serves as a pull down resistor in order to prevent unwanted LED blinking during start up of the whole system and the MCU, when there can be undefined logic levels on the output pins. The value of the resistor can be chosen as 10kΩ without second guessing it, because the main purpose is to keep the logic level on zero and it will not affect anything on the output as there are no sensitive measurements taken nowhere around the transistors.

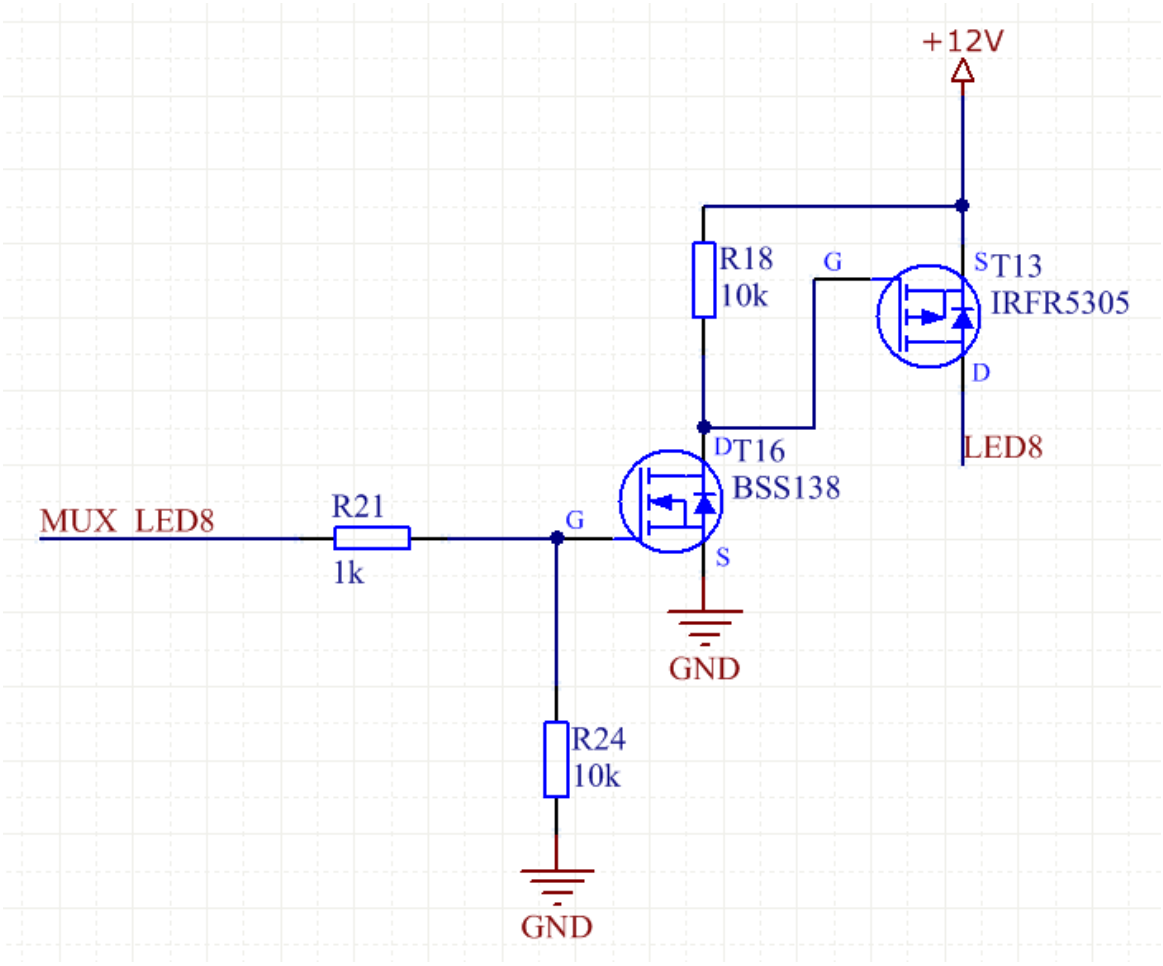

Picture 5: First version of the LED MUX part

PWMs connected to the MCU are designated R (red), G (green), B (blue), viz. Picture 6, leading to the LED connector and controlled with the software designed by our software engineer. As a checking unit, an LT6221 was incorporated, to make sure that the PWMs are working correctly. LT working as an opamp amplifies the signal and sends it back to the MCU to compare it to its inner DAC reference.

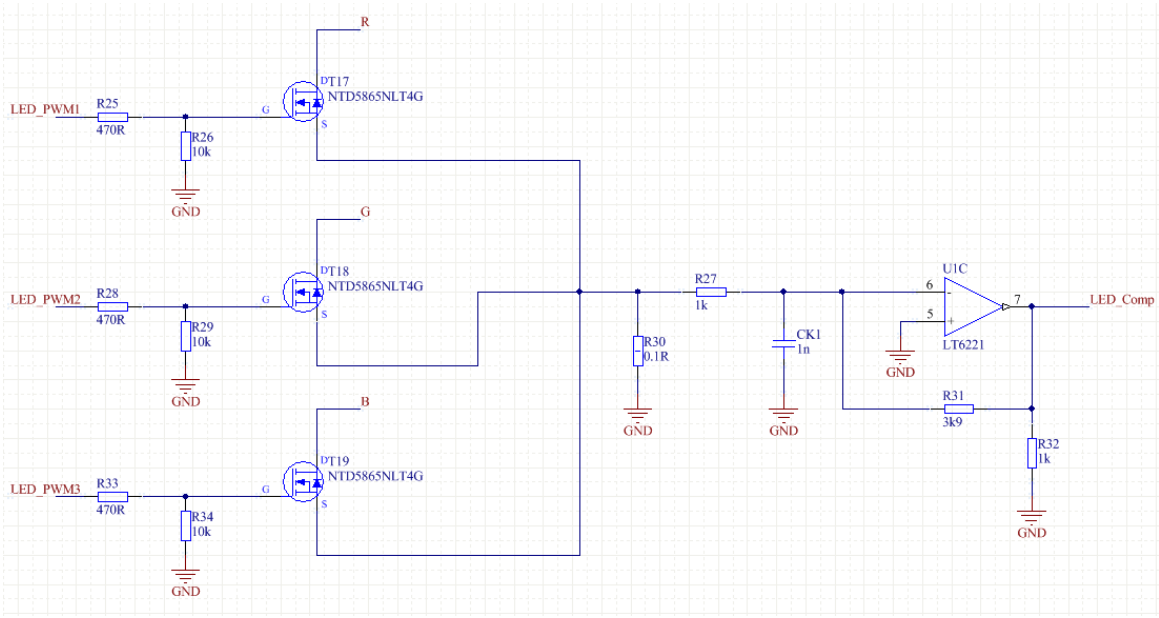

Picture 6: First version of the LED PWM part

Considering that there is certain amount of current coming out of the MCU pins, simulations had to be made to ensure acceptable power dissipation on the NTD and IRF transistors so the heat emission would not be too high. All of these were done in LTspice IV [2] and can be seen in the following Figure 5 and Picture 7, which show the values on both transistors.

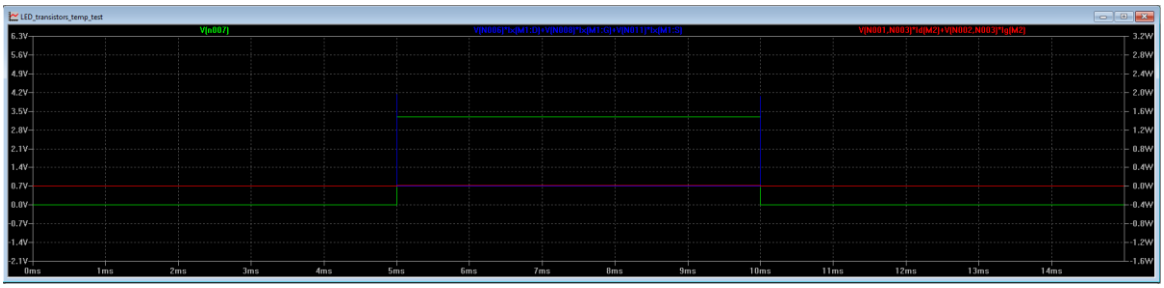

Figure 5: Power dissipation of IRF and NRD transistors (red line - IRF; blue line – NTD; green line – power supply; X axis - time [ms]; right Y axis – power dissipation [W]; left Y axis – voltage [V])

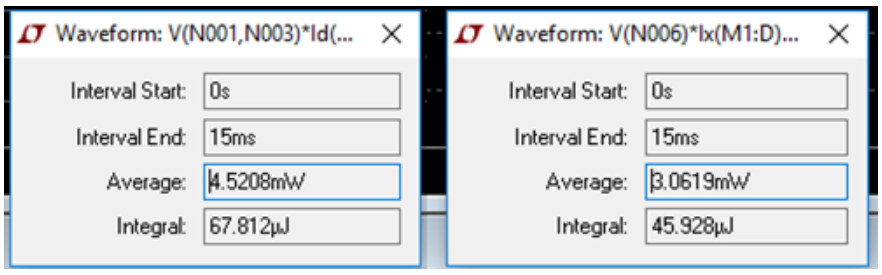

Picture 7: Transistor power dissipation in numbers (left - IRF; right - NTD)

As shown on the screenshots above, the power dissipation is safely within the acceptable range and confirms that both transistors can be used in this application. The power spikes, appearing when the MCU launches and ends the signal, last in a matter of nanoseconds and do not endanger the transistor functionality or the component itself.

Another LED schematic upgrade included an external comparator. It was not possible to use the MCU for this purpose so I decided to make a use of the second part of the LT6221. The first part now serves as an amplifier while the other part serves as a voltage comparator. But for this it first had to be verified that the LT is fast enough and can work as a comparator without slowing down the rest of the circuit or affecting its effectiveness. Using the LTspice programme, I compared one random, but fast – 500 ns, voltage comparator from the LTspice library and the LT6221. As seen in the following Picture 8 and Figure 6, the LT is actually more than sufficient for this application with the time of comparison equal to 652 ns.

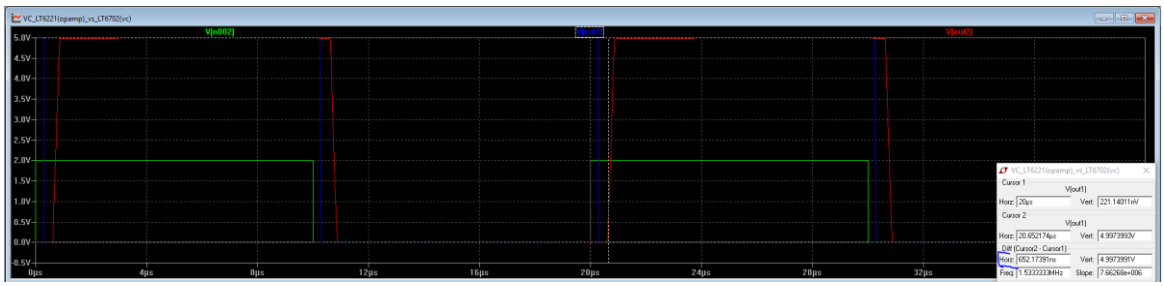

Figure 6: Switching comparison of LT6221 and a voltage comparator (blue line - comparator; red line - LT6221; green line - power supply; X axis - time [µs]; Y axis – voltage [V])

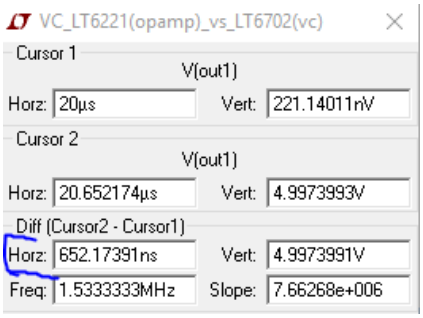

Picture 8: Table with visible numbers - speed of switching for the LT6221 component

After an update from the marketing department, the number of LED lights was increased to 17, changed to a single color and it was decided that they are going to be placed around the platform. Using three PWMs to determine the color became redundant, but also using 17 different MCU pins as a MUX was unthinkable. Another solution had to be devised. The aim was to wire all LEDs around the balancing board while using as few wires as possible, but still keep the ability to control the brightness of every single LED. Three options were considered – shift registers, external multiplexer and LED matrix. Using an external MUX was impractical, even though I would have saved the most MCU pins, it might be unnecessarily complicated. And even though the shift registers might have been the most elegant solution, there were not any available in the company database. Institution of a new part for just one project is not possible, because the process would take too long, so the only possibility left was to use a matrix. My board would include a connector, set up to create a matrix for the LED (Picture 10), which would be on their separate mini-boards, placed where they need to be. To get ahead of future changes in the number of LEDs, I used six MCU pins as a MUX, circuit example can be seen on Picture 9, and four different pins as a PWM, as seen on Picture 11. Moreover, the end branch comparator was scratched and

deleted from the design along with the IRF transistor. Everything powered by the 3.3 V (DVDD) source.

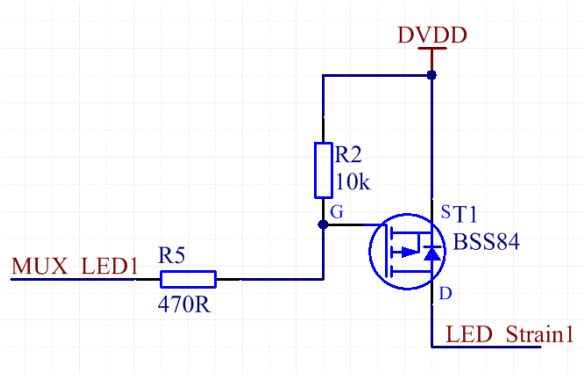

Picture 9: Final version of the LED MUX part

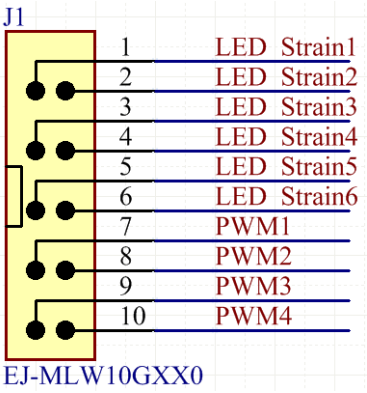

Picture 10: Connector for the LED part of the board

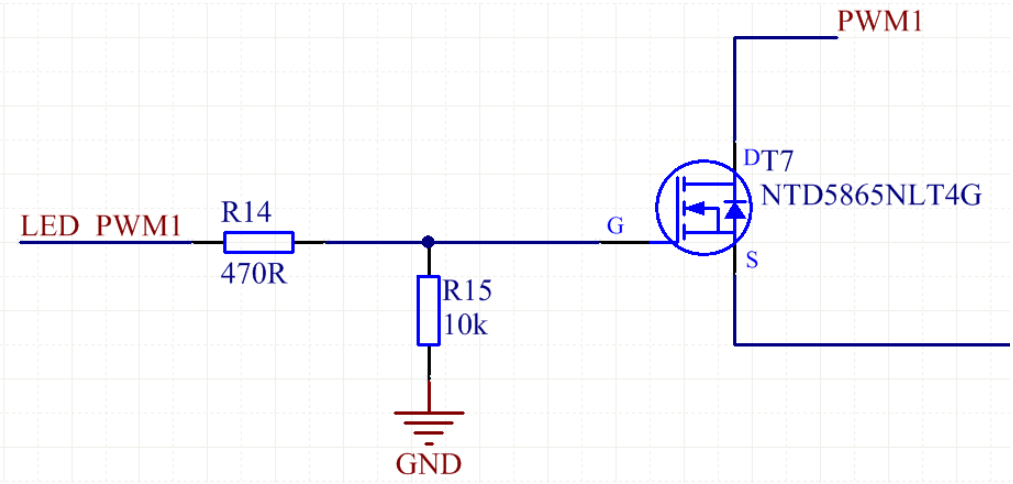

Picture 11: Final version of the LED PWM part

The R2 is working as a pull down resistor. It ensures that the LEDs will not flicker during the start up of the machine. Its value just needs to be high enough a to keep the logical value to zero, but does not have to be specifically calculated and can be set ass one of the standard values instead, because it will not affect an output of some measuring unit and the same goes for the R15 resistor. The value of R14 on the other hand had to be more specific. The

maximal current output the MCU can handle is 10 mA. The power supply is 3.3 V so a simple Ohm's law is sufficient (equation (4)).

$$R = \frac{3.3\ V}{10\ mA} = 330\ \Omega \tag{4}$$

As 330 Ω is not in the company's database a different resistor had to be used. I could not go any lower, because that could endanger the MCU so I chose the closest resistor with a higher value. Overall, this design was then authorized and is used as the final concept for the LED schematic.

3.2.5. POWER SUPPLY

Using +12V from the main (gener) board I decided to use LM1117 component as a LDO for the voltage to power most of the board – ADC, MCU, Accelerometer – (+3.3V) and the CAN communicator (+5V). On the following pictures, you can see the schematic designs of the whole power source. The LM datasheet [10] depicts the correct wiring and describes the correct equation for calculating the dropdown value.

$$V_{out} = V_{ref}\left(1 + \frac{R_2}{R_1}\right) + I_{ADJ}R_2 \tag{5} [10]$$

The second part of the equation (5) is a correction for I_{ADJ} going from the ADJ out to the rest of the circuit. V_{ref} equals to 1.25V in our case, R_2 is the resistor value in the bottom part of the voltage divider and R_1 in the upper part, I_{ADJ} is 60µA. My goal was to step down the +12V value to an approximately 3.3V (Picture 13) and 5V (Picture 14). The obstacle behind this was to choose from the resistors on stock and to use as small ohmic values as possible, so the final voltage output would not be affected by the corrective term. Even though the error introduced by the I_{ADJ} could be neglected, while using low value resistors, however, to make my calculations as accurate as possible, I included the corrective term in both of my designs.

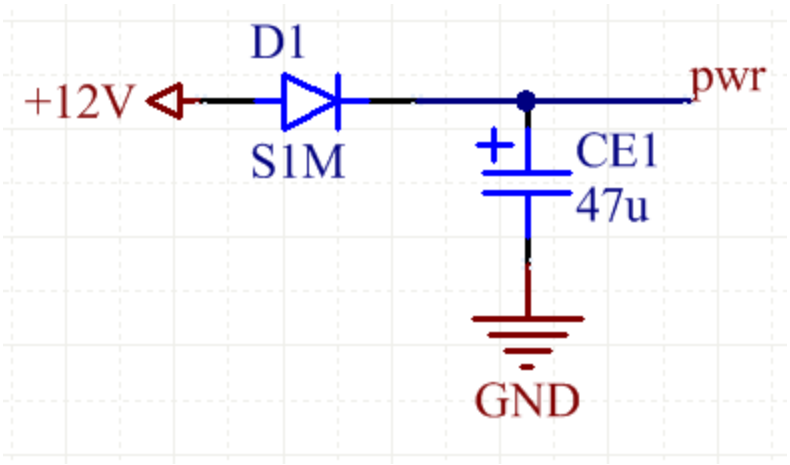

Picture 12: Pole reversion protection for the power source

As a protection against pole reversion, there is a simple diode that will stop the current from flowing the other way in case the power source got connected with incorrect polarization. Picture 12 above this paragraph shows the wiring.

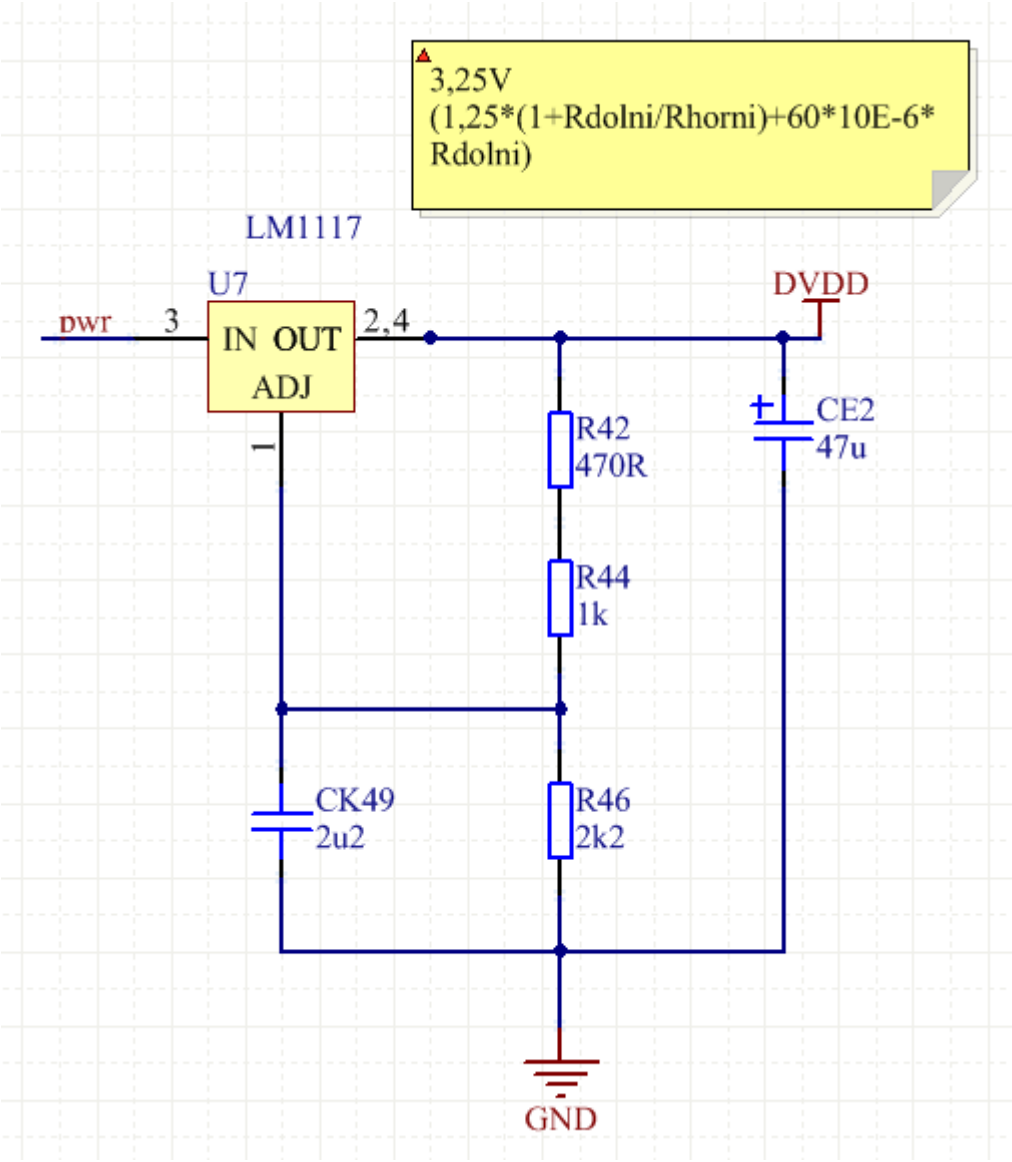

Picture 13: "3.3 V" power source branch

Capacitor values were chosen to correspond with the datasheet requirements. To improve the transient response as well as the stability of the source a 47µF tantalum capacitor was put on the output net. Another capacitor with the same value was put on the input branch. A lower capacitor would suffice for most applications [10], but a higher value does not affect the design and is available in the company's storage. To improve the PSRR [19], an ability to reject a certain amount of noise in the component, a 2.2µF capacitor was used in parallel with the second part of the resistor branch.

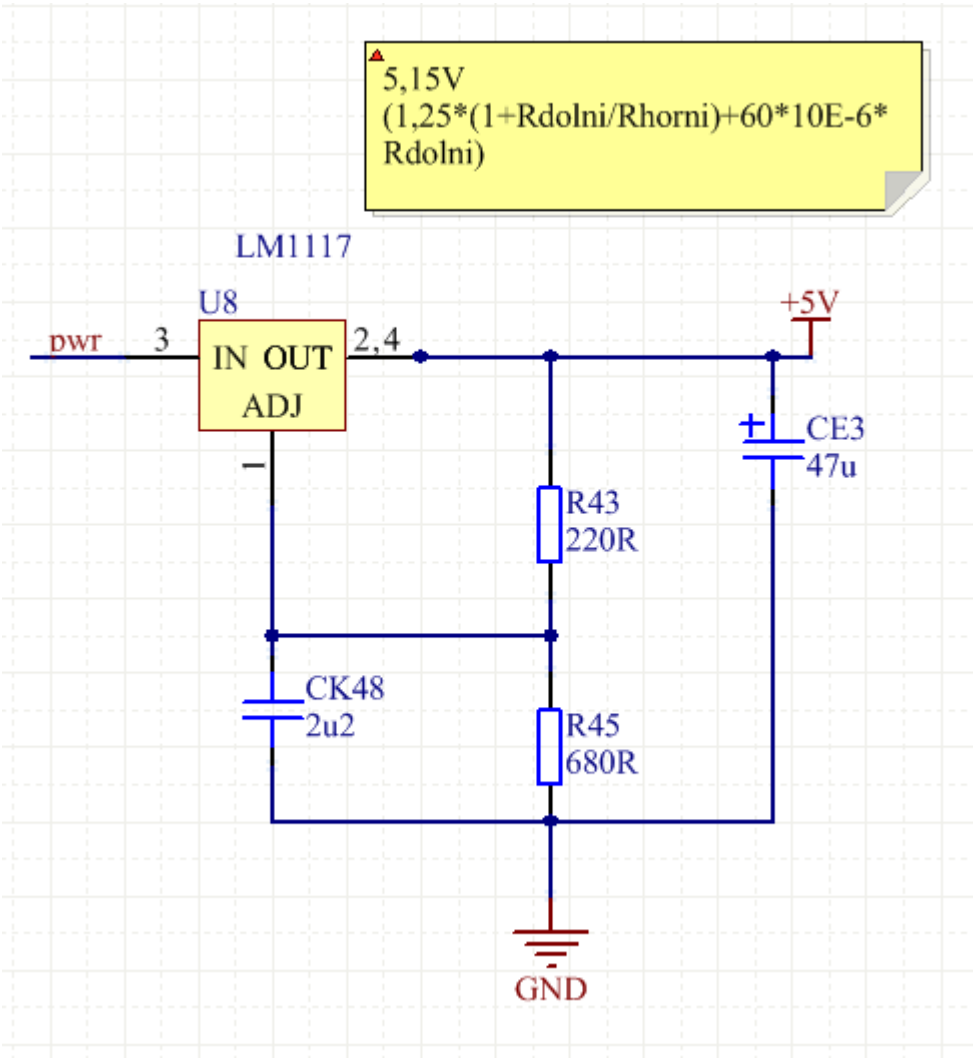

Picture 14: "5 V" power supply branch

A different +5 V power supply had to be used for load cells, because the voltage output, given by every load cell, is directly dependent on the strength of the power source. According to the LC datasheet [5], the sensitivity equals to 2 mV/V, meaning the output of every LC is 2 mV per every volt pumped into it. Simultaneously the value coming to the ADC is always compared to an inner reference. This could lead to inaccurate readings from the load cells in case of oscillations in the inner reference or the LC power supply. Therefore to ensure the stability of the power source in conjunction with the resulting data, I used the inner reference of one of the ADCs to power a small amplifying circuit, which is then used to power up the load cells. For this purpose, I used an N-channel power MOSFET NTD5865NL [12]. Creating a circuit along with LT6221 [9] operational amplifier, I managed to get a power source for the load cells That guarantees that in the event of power oscillations the output is shifted by the same amount and the data will still be relevant in connection to previous measurements. The table below depicts, how much would the output change in case of a just 0.15 V shift in the power source:

Table 5: Influence of the power supply on the LC output

Max = 200kg		
LC sensitivity - 2mv/V		
Power supply [V]	5	5.15
200kg =	10mV	10.3mV
1kg =	50uV	51.5uV
Difference	0.3mV	= 6kg

Table 5 shows that the difference by only 150 mV could change the final outcome by as much as 6 kg, which would completely ruin the diagnostic ability of the machine.

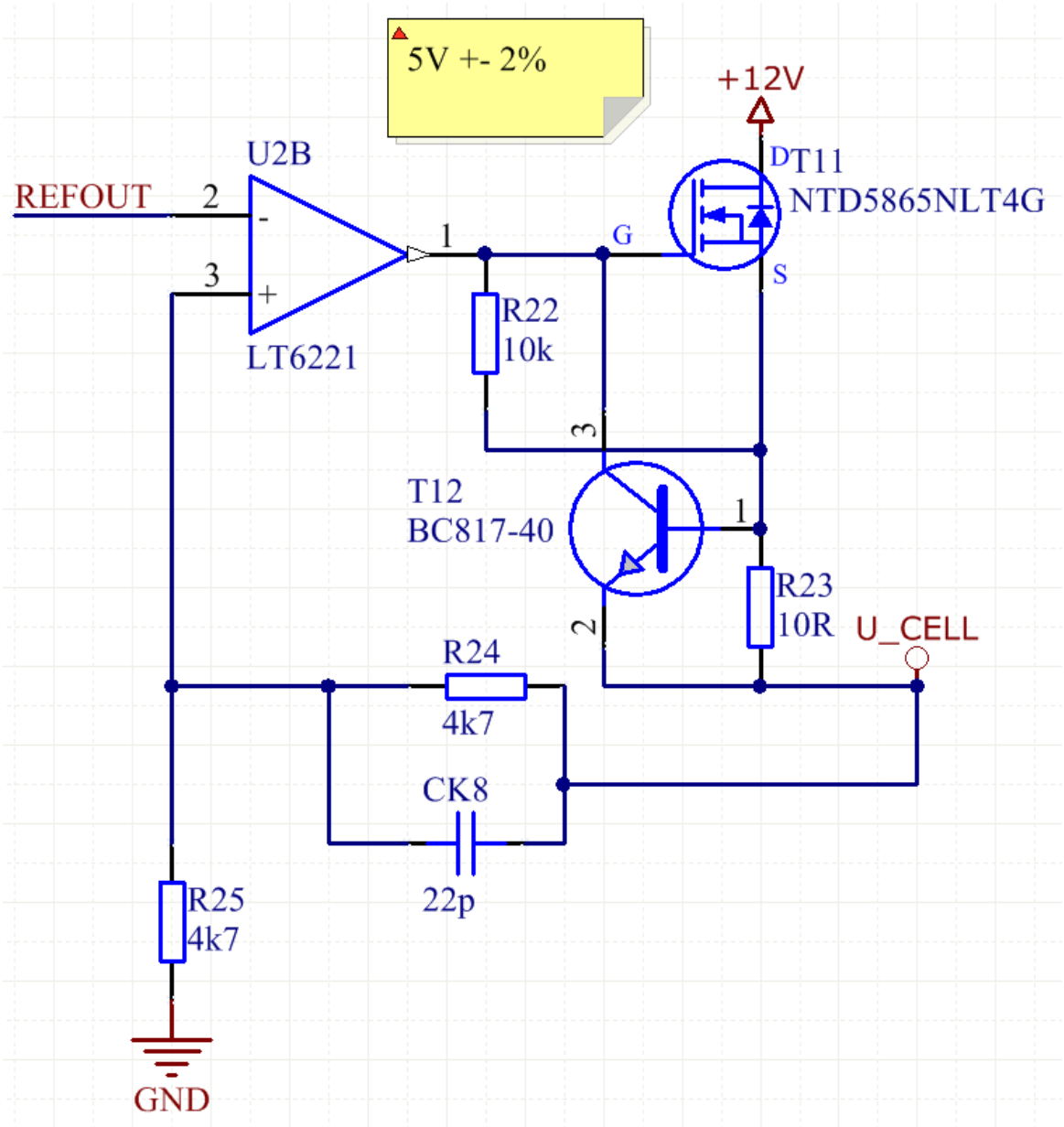

Picture 15: Special power supply circuit for load cells

Picture 15 depicts the extra load cell power supply circuit. REFOUT voltage comes from one of the ADCs, which uses it for its inner reference. Its value is approximately 2.5 V [6] and using the operational amplifier, the input is doubled. To ensure the correct working of the circuit in case of current spikes a current limiter has been included. Using the BJT (Q1) will, along with the resistors (R23, R24) and a capacitor (CK8), safeguard the load cell power source against unexpected high currents. Values of two parts had to be tuned, otherwise their influence on the circuit would distort the power source stability. For that I used LTspice [2]. I recreated my circuit, using the same part that were supposed to be in the final schematic of my board. To begin with, I had to overcome certain shortcomings of the LTspice, the libraries. Even though there is a vast variety of components, the transistor, NTD5865NL, I needed, was not among them. Therefore it was up to me to create a new LTspice component. Using its datasheet [12] and a datasheet archive [20] I found out and calculated the most important parameters and input them into a new LTspice transistor. ... After that, I could begin working with LTspice. To most effectively compare the possibilities, I used the command line in the programme and the *step param* directive, with various parameters. And the *DC sweep* command allowed me to test the workings of the current limiting circuit and confirm that the values and the wiring is correct.

Now we will focus on the parameters. Firstly the capacitors value, 100 pF is usually used in current limiters, its capacitance has a direct impact on the initial power supply startup (in other word, how long does it take for the power supply to stabilize on our desired 5 V value). Using a smaller value decreases the startup time by half, as seen in the Figures 7 and 8 below, and therefore I decided to implement a 22pF capacitor. That altogether speeds up the machine's ability to measure and eliminates false values that could be caused by power source spikes in LCs.

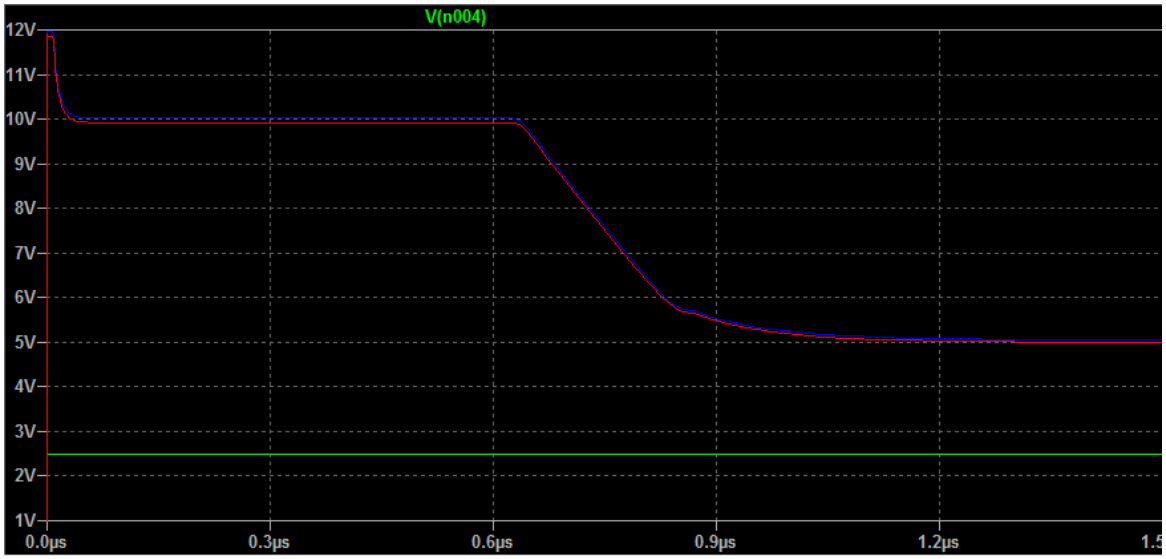

Figure 7: Stabilization of the power supply with 22pF capacitor (X axis - time [µs]; Y axis - voltage [V])

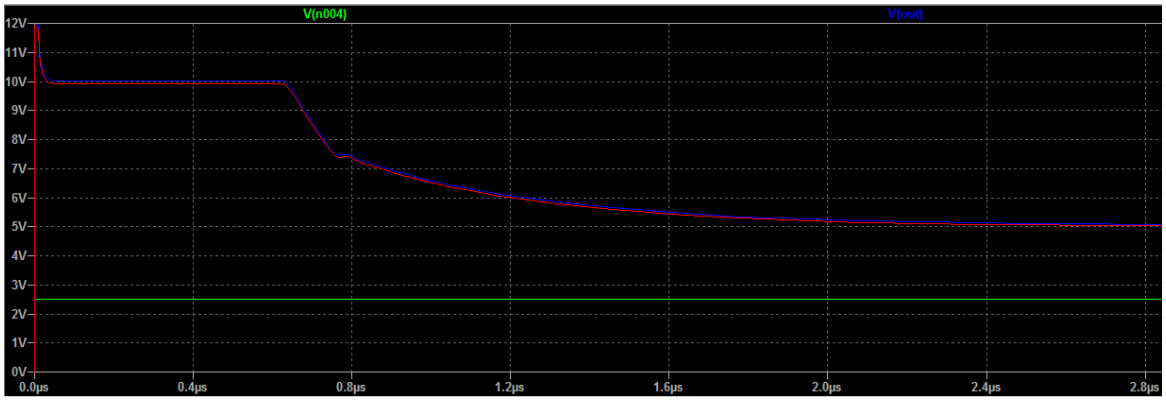

Figure 8: Stabilization of the power supply with 100pF capacitor (X axis - time [µs]; Y axis - voltage [V])

Secondly a value of the R23 resistor. To correctly limit the current up to a maximum of 100 mA, the resistor should be around 10 Ω, as shown in the equation (6) below. A higher resistor would work as well, but is not available in the storage. And considering that the load cells will drain a maximum of 10mA, this current limitation is more than sufficient and will not affect the function.

$$I = \frac{0.65\ V}{10\ \Omega} = 65\ mA \tag{6}$$

Another aspect was the power dissipation on the resistor so it would not heat up too much and cause voltage fluctuations in the power supply. But as seen in the following Picture 16, the power dissipation is not problematic in our application.

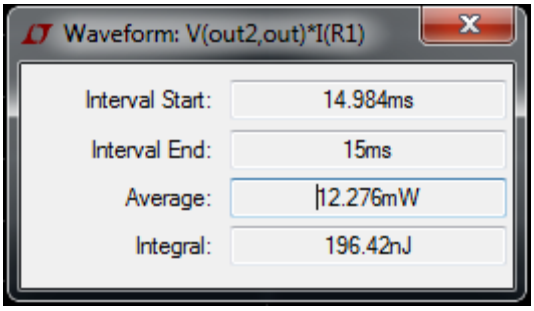

Picture 16: Power dissipation on the R23 resistor

Two other schematic parts on Picture 17 depict the power source for the opamp and the wiring for the other part of the LT component in order to prevent abrupt voltage changes caused by undefined values on the inputs.

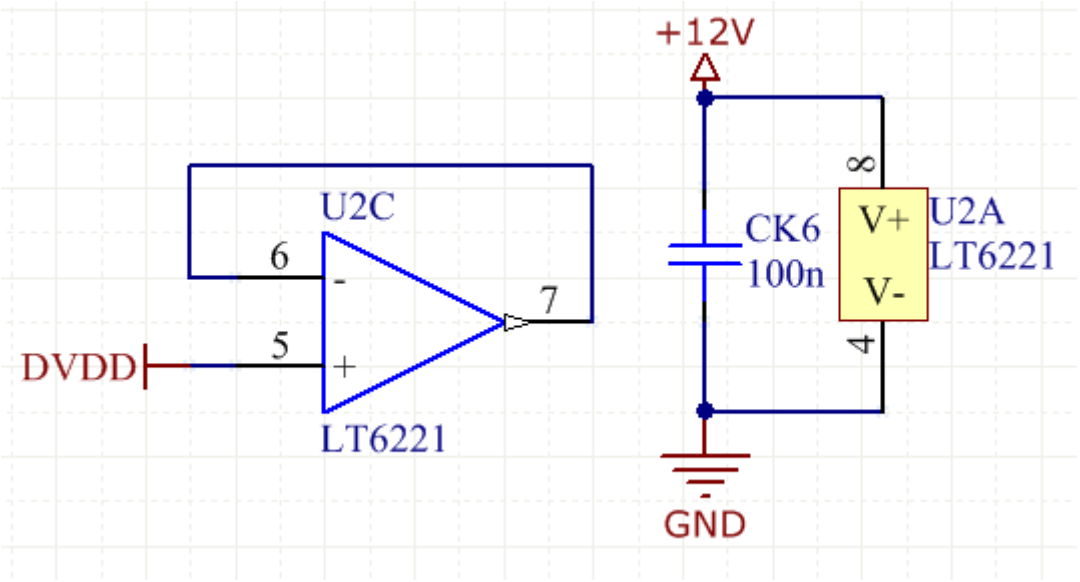

Picture 17: The rest of the LT6221 circuit

3.2.6. CAN COMMUNICATION

As a communication channel to connect the Core LC board and the platform main board a CAN was deemed to be the best. MCP2561/2 CAN Transceiver [21] is well suited for my board due to its compatibility with 12 V or 24 V systems. Many different parts and boards in the stabilizing machine are powered by 12 V (24 V) so the transceiver fits with the rest. The wiring itself on Picture 18 is compatible with what is shown in the datasheet, but the CAN connector was also used to lead the higher voltage to the whole board. To be more precise, to supply the power source related part of the board, which then lowers the voltage to a desired values that are used to power the rest of the design.

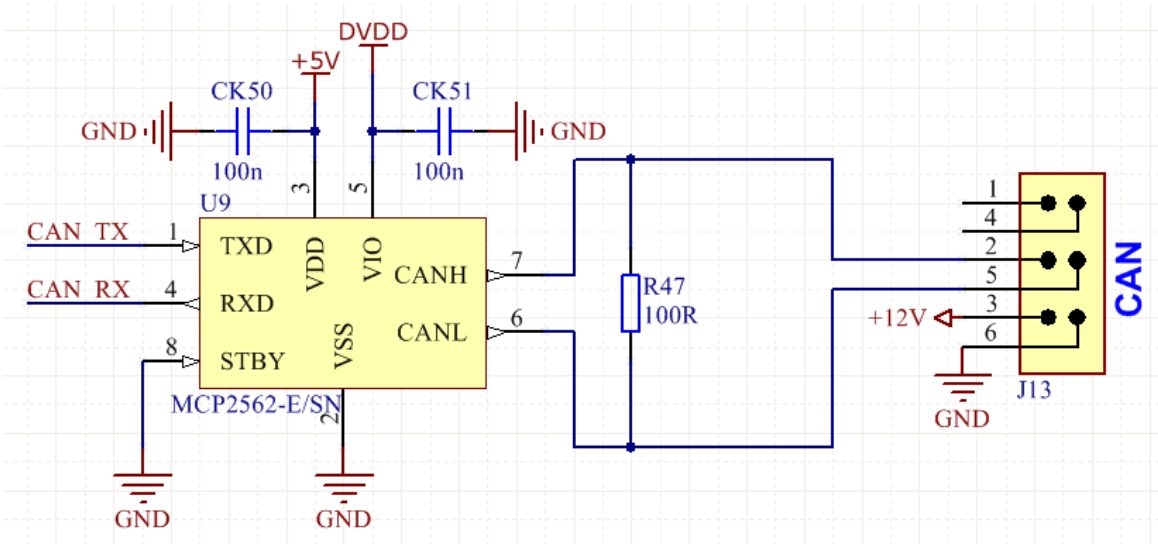

Picture 18: CAN communicator and connector wiring

4. CONSTRUCTION AND TESTING

The rest of the schematics, which were not shown in the rest of the thesis, or the schematic as a whole, can be seen in the appendix on the enclosed CD [Appendix A].

4.1. PCB DESIGN IN ALTIUM

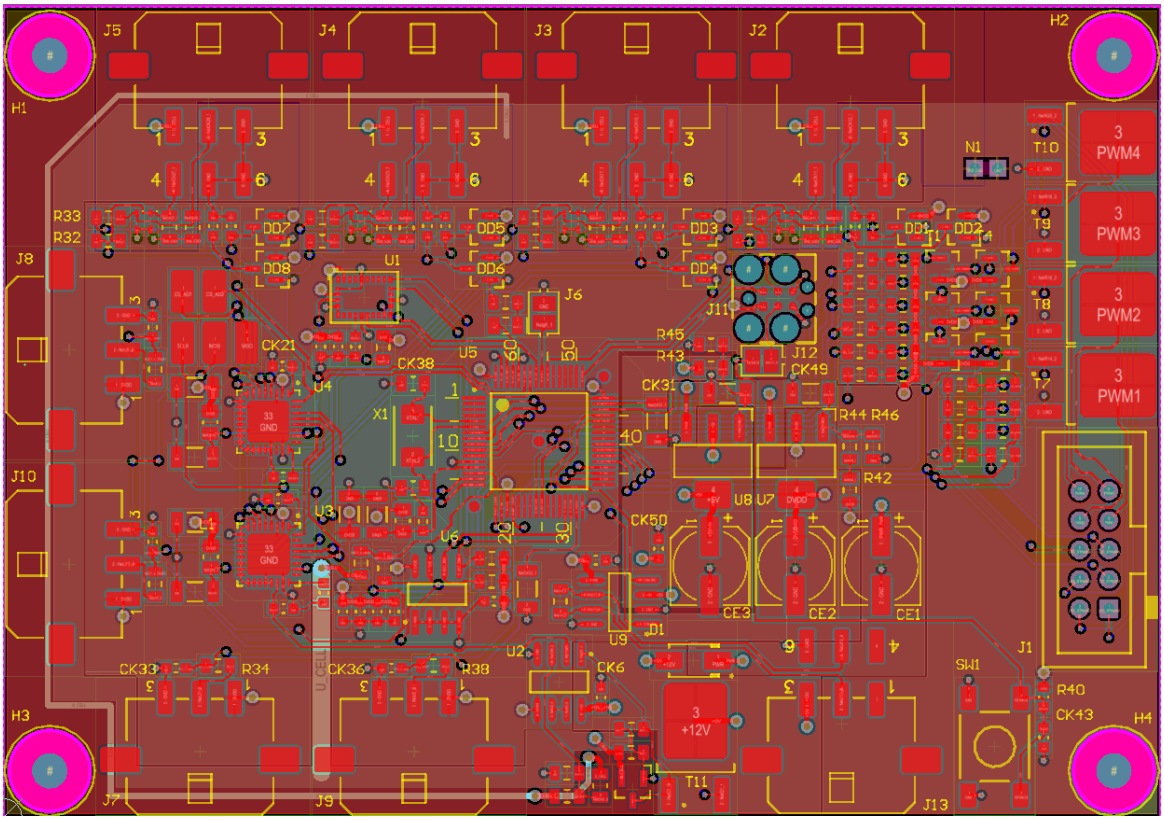

Picture 19: 2D PCB design

The final layout of the board is depicted in the Picture 19 above. Connectors located on the sidelines of the board, MCU handling everything from the middle and other parts placed in order to follow certain rules. To avoid basic mistakes during the design, I searched for information on this matter. For example methods to keep from creating redundant magnetic field disturbances, which could negatively affect the board and might interfere with other parts of the machine or the best way to lead paths on the board, where to place capacitors and overall to create a clean layout of the board. Most of these information I found in the book [22]. And for a better visualization, Picture 20 shows a 3D layout of the board.

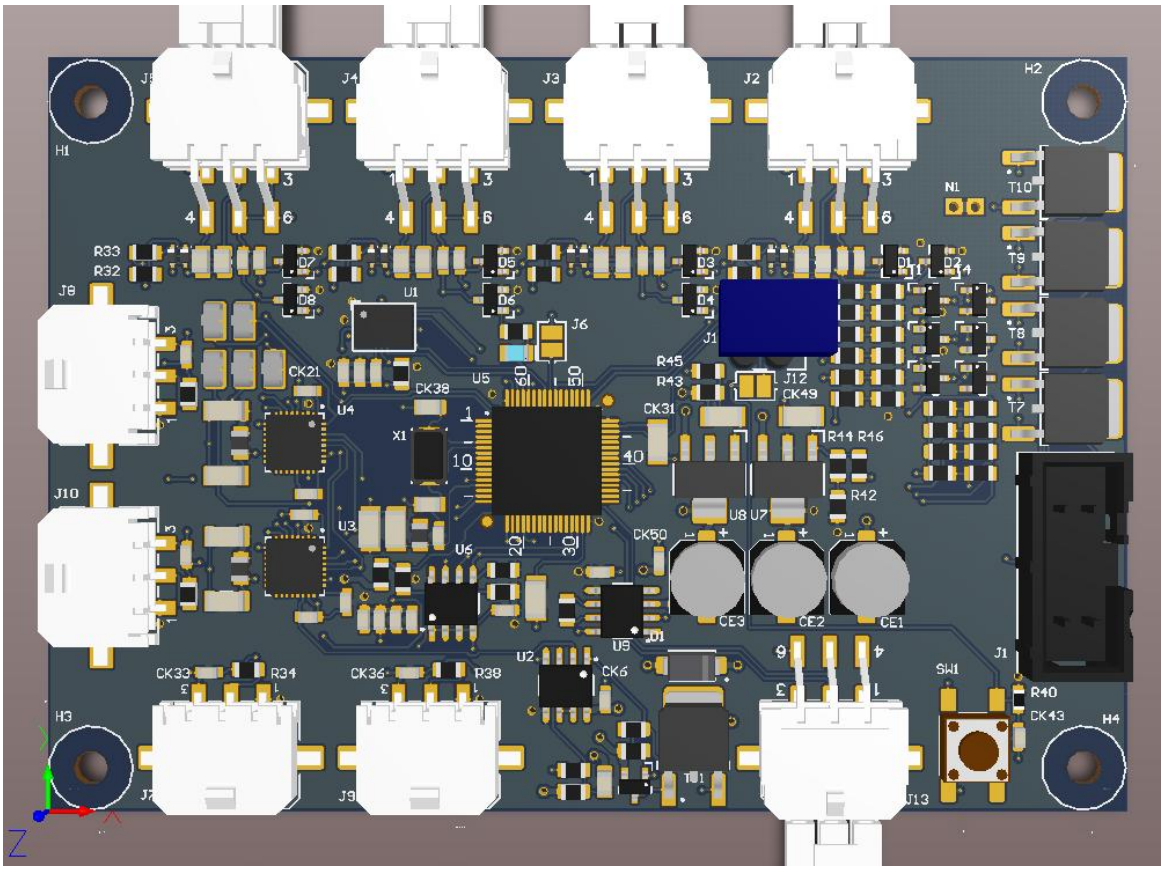

Picture 20: 3D PCB design

The biggest challenge in the PCB design was fitting all of the parts on a relatively small board with given height and width parameters, which could not be changed due to a limited free space between the parts in the machine. The final count is 162 components, consisting of connectors, resistors, capacitors, LDOs, ADCs and many others (specific number can be seen in appendix [Appendix B]. All of the connectors had to be on the side of the board, so they would not consume too much unnecessary space when connected to a cable. I also had to keep in mind the layout of the circuit. The stabilizing capacitors had to be as close to the LDO as possible. The same rule is applied to every capacitor, the component should be as close to the part it is supposed to affect as the design allows. To avoid unnecessary losses with pathways on the surface, it is better to use more vias to connect to the ground layer.

The ground layer consists of two parts. The regular ground polygon, which takes up most of the board and then an ESD part, spread only under the parts, which needed the ESD protection – the LC connectors. These two layers are connected in a single node.

Power supply layer (Picture 21) is a little bit more divided. There is the high voltage coming through the CAN connector, 3.3 V for most of the board, 5 V for the CAN itself and a different 5 V for the LCs. The load cell branch is however a little bit different. Part of it is specifically lead from the R and C parallel to avoid losses on the line. Using an online calculator and specific parameters (width of the path, length, parameters of the material, ...) I determined the voltage drop that would have otherwise occurred. Resistance of the path would be around 0.035 Ω and there is approximately 0.04 A going through it. Even though it

would have been around 1 mV drop per roughly 13 cm of the line, it is still an unwelcomed change in the power supply we would rather avoid.

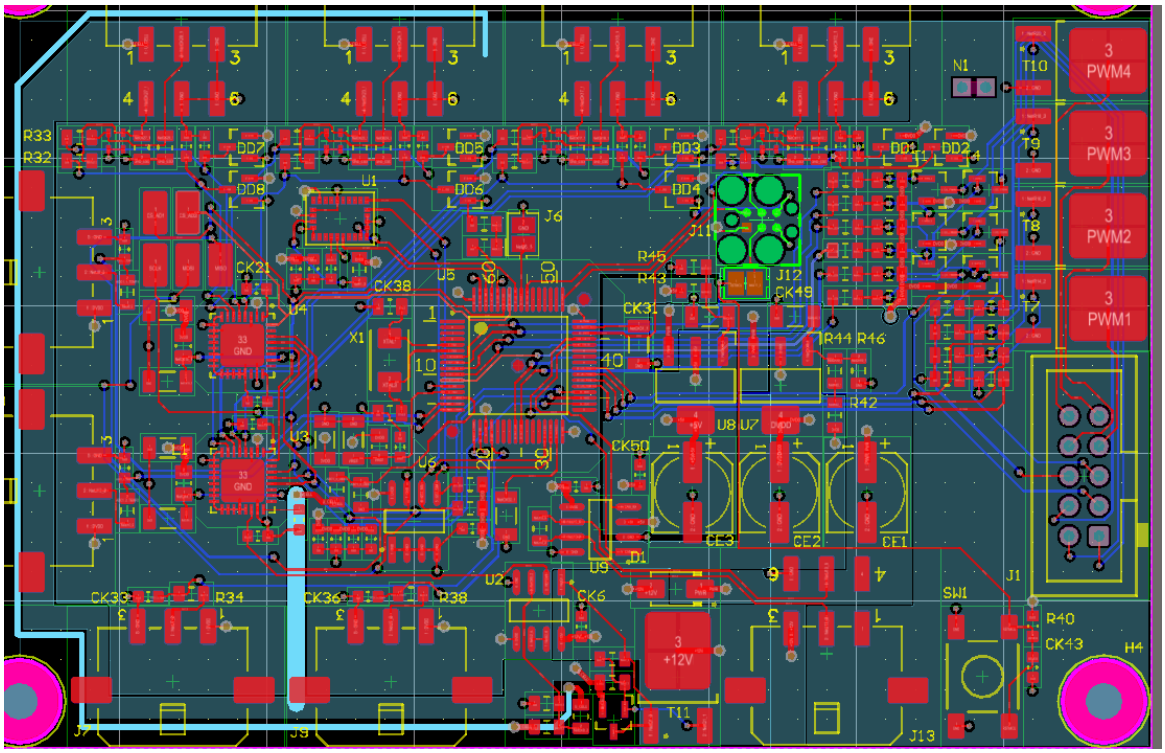

Picture 21: PCB design of the power supply layer

4.2. MANUFACTURING PROCESS

Considering the first board was just a prototype, it was decided that I will solder the whole board by hand. That allowed me to not completely abide the set borders of the components, which would otherwise be needed for the fitting machine to set up the board correctly. This saved me some space during the design, even though I had to deal with the deficiency of space, while soldering. The biggest obstacle was watching out for bridges that could be unintentionally created as a result of a lack of space between pins or pads on the board.

4.3. REAL TIME PRODUCT TESTING

I used Bode-100 [23] testing machine from Omicron Lab [24] to test reflections after passing through the LDO for both, 5 V and 3.3 V branches. The base impedance of the measuring cable was 50 Ω and the whole machine was set according to the manual [23]

I experimentally added different capacitors in the series with the 47µF capacity to see, whether it changes the output reflection characteristics. Another test was changing the resistors, which are used to generate the desired voltage. The result, as seen below, is that my LDO (LM1117) is almost impervious to the changes I made to the circuit. The flow of the line is, except a little offset, almost the same and that goes for both, the 3.3 V as well as the 5

V power source. The jitter in the beginning is caused by random noise in the signal. I used Matlab to portray Figure 9, which displays my measurements.

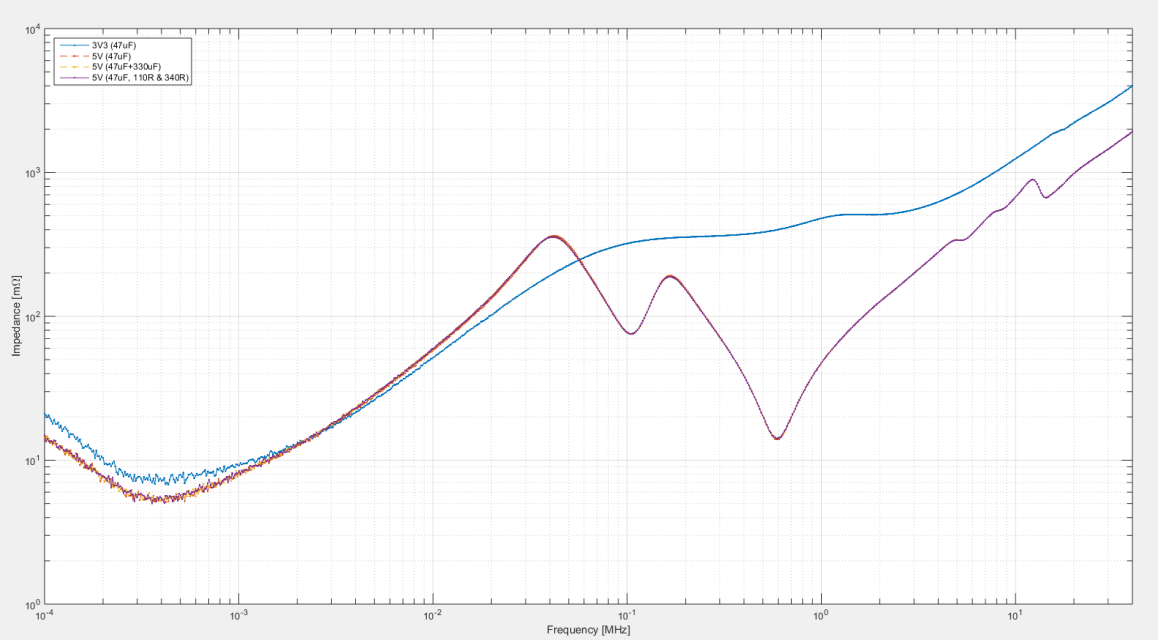

Figure 9: Course of the BODE measurement (Blue line - 3.3 V; red stripes – 5 V; yellow stripes - 5 V with added C; purple line – 5 V with added R; X axis – log frequency [MHz]; Y axis – Impedance [mΩ])

Ideally, the line would be pretty much a constant, but to achieve that, I would have to have various capacitors of all values spread across the whole board. But in my case, different depressions in the graph are cause by different capacitors. The 2.2µF can be seen around 600 kHz, the 100nF would be between 5 MHz and 6 MHz, while the 47µF is probably the very first one. The rest of the depressions might be caused by some contaminant on the board, an error or something else on the board. It could also be cause by some random sum of multiple capacitors. Nevertheless, from the figure above arises that the LDO is so good, it cannot be modulated by added components. The only way to alter it would probably be via current feedback. And to my advantage, all of my components are using low frequencies, so the rising impedance in the matter of megahertz is not an issue and the tests were successful.

One of the most important tests was to confirm that the filter that had been chosen and the number of ADCs can actually deliver the results, which are needed for the balancing platform to perform correctly. The board was connected via programming unit to the computer, a new binary file with rewritten pins was imported and the measurements, which had to be undertaken at the very beginning, were done again the same way. Through the STM Studio I confirmed that the peak-to-peak noise is even a little lower than with the previous board version and therefore fits our application without a hitch and due to this the desired resolution is reached, meaning the peak to peak noise is less than 25 g. And even though the chosen number of ADCs and the filter does not fulfill the SPS parameter, it is still high enough that the balancing platform is capable of processing the data fast enough and it will not affect its functionality.

5. CONCLUSION

The board as a whole fulfils the requirements listed in the assignment and the whole process forced me to overcome various issues and difficulties I met during its creation. I learned methods to design and effectively test circuits in a more complex architecture, which the board represents, along with confirming that the design that had been created works in real world application.

All of the parameters set in the task were met, even though some had been adjusted, nevertheless, none of them affect the overall functionality of the balancing platform. The final noise measurements were around 400 units of raw value, which is more than satisfactory, and can be further improved by working with software averaging and other methods. That means that I was able to meet the peak to peak noise requirement, which is lower than 25 g. And as was shown in the very beginning of this thesis, the final ADC noise value could even be a little higher, so occasional noise spikes should not even affect the results. Moreover the ADC can work as fast as 160 samples per second, which is lower than what was set by the assignment, but is more than sufficient for the correct working of the machine. And considering it allows for lower noise, which is in this case a superior parameter in comparison to sampling speed, it is not an obstacle. For the last parameter, the resolution is 0.023 g/LSB, which is even better than initially expected and serves the board's purpose perfectly.

The final costs of the board (excluding VAT, for the company and including the price on agreement) are 1 858,88 CZK. The whole calculation can be seen in the appendix [Appendix B]. This concludes that the price is way favorable than construction from separate parts (exemplary figures for one of the board functions were showed in Table 2).

Overall, the board was a success and is ready to be used for real time application as a collecting and controlling unit in the stabilizing and balancing platform in BTL development, for which it was designed for.

BIBLIOGRAPHY

[1] A. LLC, "Altium Designer," Altiumm LLC, 2017. [Online]. Available: http://www.altium.com/altium-designer/overview. [Accessed January 2017].

[2] L. Technology, "Linear," Analog Devices, 2017. [Online]. Available: http://www.linear.com/designtools/software/. [Accessed January 2017].

[3] STMicroelectronics, "STM Studio," STMicroelectronics, 2017. [Online]. Available: http://www.st.com/en/development-tools/stm-studio-stm32.html. [Accessed January 2017].

[4] STMicroelectronics, "ST-LINK," STMicroelectronics, 2017. [Online]. Available: http://www.st.com/en/development-tools/st-link.html. [Accessed January 2017].

[5] Z. Europe, "DATASHEET - L6E load cell," June 2010. [Online]. Available: http://canvina.com/upload/download/L6E.pdf. [Accessed January 2017].

[6] A. Devices, "DATASHEET - AD7124-8," 2015. [Online]. Available: http://www.analog.com/media/en/technical-documentation/data-sheets/AD7124-8.pdf. [Accessed January 2017].

[7] Bosch Sensortec GmbH, "DATASHEET - BNO055," November 2014. [Online]. Available: https://cdn-shop.adafruit.com/datasheets/BST_BNO055_DS000_12.pdf.

[8] STMicroelectronics, "DATASHEET - STM32F405xx," 2015. [Online]. Available: http://www.farnell.com/datasheets/1994630.pdf?_ga=1.18515833.19875267.1473930790. [Accessed January 2017].

[9] Linear Technology, "DATASHEET - LT6220/LT6221/LT6222," 2003. [Online]. Available: http://cds.linear.com/docs/en/datasheet/622012fc.pdf. [Accessed January 2017].

[10] T. Instrument, "DATASHEET - LM1117," January 2016. [Online]. Available: http://www.ti.com/lit/ds/symlink/lm1117.pdf. [Accessed January 2017].

[11] F. -. O. Semiconductor, "DATASHEET - BSS84," February 2013. [Online]. Available: https://www.fairchildsemi.com/datasheets/BS/BSS84.pdf. [Accessed January 2017].

[12] O. Semiconductor, "DATASHEET - NTD5865NL," September 20104. [Online]. Available: http://www.onsemi.com/pub/Collateral/NTD5865NL-D.PDF. [Accessed January 2017].

[13] F. -. O. Semiconductor, "DATASHEET - BSS138," October 2005. [Online]. Available: https://www.fairchildsemi.com/datasheets/BS/BSS138.pdf. [Accessed January 2017].

[14] The Eclipse Foundation, "Eclipse," The Eclipse Foundation, 2017. [Online]. Available: https://eclipse.org/. [Accessed January 2017].

[15] STMicroelectronics, "STSW-STM32095," STMicroelectronics , 2017. [Online]. Available: http://www.st.com/en/development-tools/stsw-stm32095.html. [Accessed January 2017].

[16] Tag-Connect, "Tag-Connect," Tag-Connect, LLC., 2017. [Online]. Available: http://www.tag-connect.com/TC2030-MCP. [Accessed April 2017].

[17] S. Corporation, "What is frequency at load capacitance?," [Online]. Available: http://www.statek.com/pdf/tn33.pdf. [Accessed January 2017].

[18] T. -. Q. Crystals, "SMD GLASS CRYSTAL 7A SERIES," [Online]. Available: http://www.txccrystal.com/images/pdf/7a.pdf. [Accessed January 2017].

[19] Editorial Team, "All about circuits - Understanding Noise and PSRR in LDOs," © EETech Media, LLC, 16 June 2015. [Online]. Available: https://www.allaboutcircuits.com/technical-articles/understanding-noise-and-psrr-in-ldos/. [Accessed April 2017].

[20] D. Archive, "ntd5865nl.sp2," Datasheet Archive, 4th April 2011. [Online]. Available: http://www.datasheetarchive.com/files/on_semiconductor/simulation-models/ntd5865nl.sp2. [Accessed 12 2016].

[21] Microchip, "DATASHEET - MCP2561/2," 2013. [Online]. Available: http://ww1.microchip.com/downloads/en/DeviceDoc/20005167C.pdf. [Accessed January 2017].

[22] C. Ing. Vít Záhlava, Návrh a konstrukce desek plošných spojů - Principy a pravidla praktického návrhu, Praha: BEN - technická literatura, 2010.

[23] O. Lab, "User Manual - Bode 100," 2010. [Online]. Available: https://www.omicron-lab.com/fileadmin/assets/manuals/Bode_100_Manual_AE4_HR.pdf. [Accessed March 2017].

[24] O. Lab, "Omicron Lab - Smart Measurements Solution," Omicron Lab, 13 April 2017. [Online]. Available: https://www.omicron-lab.com/. [Accessed March 2017].

[25] D. M. Stefanescu, "3.4 Strain Gauges," in *Handbook of Force Transducers: Principles and Components (ISBN-13: 978-3662506844)*, Springer, 2016.

[26] D. M. Stefanescu, "19. Strain Gauges Electronic Circuits," in *Handbook of Force Transducers: Principles and Components (ISBN-13: 978-3662506844)*, Springer, 2016.

[27] D. M. Stefanescu, "18. Wheatstone Bridge," in *Handbook of Force Transducers: Principles and Components (ISBN-13: 978-3662506844)*, Springer, 2016.

[28] D. Fitzpatrick, Implantable Electronic Medical Devices (ISBN-13: 978-0124165564), Academic Press; 1 edition, 2014.

[29] B. Bergeron, "Chapter 3: Digital Bathroom Scale," in *Teardowns: Learn How Electronics Work by Taking Them Apart (ISBN-13: 978-0071713344)*, McGraw-Hill Education TAB; 1st edition, 2010.

LIST OF FIGURES

LIST OF PICTURES

LIST OF TABLES

APPENDIX Ax (On CD)

Appendix A contains all of the schematics making up the board architecture.

- **A1** ACCELEROMETER.SchDoc – BNO055 circuit
- **A2** CAN.SchDoc – CAN communication with the main power supply from the rest of the machine
- **A3** LED.SchDoc – Connectors for LED making up a matrix
- **A4** LOAD_CELLS.SchDoc – LC circuits with wired ADCs, test points and the amplifying circuit
- **A5** MAIN.SchDoc – The main schematic layout
- **A6** MCU.SchDoc – MCU with ping mapping, external crystal and connectors for the programming unit and heat sensors
- **A7** PWR_SUPPLY.SchDoc – Power supply designs for 5 V and 3.3 V

APPENDIX B

This table contains the costs of separate components and the final list of all components used on the board along with the final price the company will have to pay per board.

Description	Quantity	Value	KK	Price [Kc/pc]	Price [Kc]
Low ESR, Al Electrolytyc Capacitor	3	47u	ECE+47U35VXXM	0.81	2.43
MLCC, Size 0603, 100nF/50V, X7R	30	100n	ECK+100N50V0603XXK	0.04	1.2
MLCC, Size 1206, 2u2/50V, X7R	10	2u2	ECK+2U250VXXK	0.88	8.8
NP0	1	22p	ECK+100P50VXXJ	0.04	0.04
MLCC, Size 0805, 2.2nF/50V, NP0	8	2n2	ECK+2N250VXXJ	0.21	1.68
NP0	2	22p	ECK+22P50VXXJ	0.04	0.08
General Purpose Rectifier 1A/1000V	1	S1M	ED+S1MXX0	0.35	0.35
Dual High-speed switching diodes	8	BAV99	EDD+BAV99XX0	0.19	1.52
Blue LED, 0805	1		EDL+SMDBLUEXX0	4.4	4.4
Capacitance bidirectional ESD proc c	8	5V TVS	ED+ESD5V0XX0	0.67	5.36
IDC Male Header for PCB 2x5 Pin	1		EJ-MLW10GXX0	0.95	0.95
Micro-Fit 3.0 Header, SMT	5		EJ+W4230-06PDDGBRRXX0	10.9	54.5
Micro-Fit 3.0 Header, SMT	4		EJ+W43650-0312XX0	7.75	31
Multilayer SMD Ferrite 1500R/100MH	3	1500R/100MHz	EL+JCB09152XX0	0.3	0.9
NPN, general-purpose transistor, 45	1	BC817-40	ET+BC817-40XX0	0.29	0.29
Thick Film resistor 0805 Size, 10k	12	10k	ER+10K0.1WXXF	0.02	0.24
	11	470R	ER+470R0.1WXXF	0.02	0.22
Thick Film resistor 0805 Size, 4k7	5	4k7	ER+4K70.1WXXF	0.02	0.1
Thick Film resistor 0805 Size, 1k	13	1k	ER+1K0.1WXXF	0.02	0.26
Thick Film resistor, Size 0603, 10k	1	10k	ER+10K0.1W0603XXF	0.02	0.02
	1	47R	ER+47R0.1WXXF	0.02	0.02
Thick Film resistor 0805 Size, 220R	1	220R	ER+220R0.1WXXF	0.02	0.02
	1	680R	ER+680R0.1WXXF	0.02	0.02
	2	2k2	ER+2K20.1WXXF	0.02	0.04
Thick Film resistor 0805 Size, 100R	1	100R	ER+100R0.1WXXF	0.02	0.02
	1	3k9	ER+3K90.1WXXF	0.02	0.02
Tactile switch, 6x6mm, 5mm Height	1		ESW+LSH1301XX0	1.35	1.35
P-MOSFET, Logic Level	6	BSS84	ET+BSS84XX0	0.55	3.3
N-MOSFET, Power, 60V/46A/0.016Oh	5	NTD5865NLT4G	ET+NTD5865NLT4GXX0	4.44	22.2
SMD Testpoint	5		EJ+TESTPOINTXX0	2.34	11.7
785 - Intelligent 9-axis	1	BNO055	EU+BNO055XX0	213.46	213.46
Dual 60MHz, 20V/µs, Low Power	1	LT6221	EU+LT6221CS8XX0	53.41	53.41
095 - 8-Channel, Low Noise, Low oer	2	AD7124-8	EU+AD71248XX0	162	324
095 - ARM Cortex-M4 32-bit MCU	1	STM32F405RGT6	EU+STM32F405XX0	258.58	258.58
64K I2C Serial EEPROM, SOIC-8	1		EU+24LC64XX0	2.7	2.7
Adjustable, Low-Dropout Lin Reg	2		EU+LM1117ADJXX0	9.13	18.26
095 - High-Speed CAN Transceiver	1	MCP2562-E/SN	EU+MCP2562XX0	19.2	19.2
8MHz Crystal Unit, SMT, 7A	1	8MHz	EX+8.000MXX1	11.24	11.24
Výroba PCB	1	(100x70)mm		805	805
				FINAL PRICE:	1858.88

APPENDIX C

Different number of ADCs + different filters, with all SPS measurements.

FULL PWR MODE + GAIN128 + 3,3V										
LCs	ADs	Filter	Filter nr.	MIN	MAX	Noise (var)	SPS - theor (1LC)	SPS - theor (ALL)	SPS - real (1LC)	g_nTenzCyclesCounter7124 [Sa]
1	1	$sinc^3$ - bez PE	1	8394200	8412000	17800	19200	19200	19282.55	19282.55
1	1	$sinc^3$ + PE	1	8556000	8572500	16500	19200	19200	19282.7	19282.7
1	1	$sinc^3$	80	8557550	8558050	500	240	240	242.05	242.05
1	1	$sinc^3$	20ZL	8557200	8557870	670	320	320	322.4	322.4
1	1	$sinc^4$	60	8557560	8558050	490	320	320	322.35	322.35
1	1	$sinc^4$	15ZL	8557470	8558170	700	320	320	322.25	322.25
2	1	$sinc^3$ - bez PE	1	8547000	8566300	19300	3200	6400	2449.075	4898.15
2	1	$sinc^3$	20	9915410	9915840	430	160	320	158.825	317.65
2	1	$sinc^3$	10	8557410	8558120	710	320	640	312.125	624.25
2	1	$sinc^4$	15	9911240	9911700	460	160	320	158.8	317.6
2	1	$sinc^4$	8	8557380	8558180	800	300	600	293.25	586.5
2	1	FSM $sinc^{3+1}$	2	8557420	8558130	710	266.665	533.33	261.5	523
2	1	FSM $sinc^{4+1}$	2	8557470	8558120	650	252.63	505.26	248.1	496.2
REZISTOR - WHEATSTON										
FULL PWR MODE + GAIN128 + 2,5V										
LCs	ADs	Filter	Filter nr.	MIN	MAX	Noise	SPS - theor (1LC)	SPS - theor (ALL)	SPS - real (1LC)	g_nTenzCyclesCounter7124 [Sa]
2	1	$sinc^4$	8	1.1E+07	1.1E+07	500	300	600	293.5	587
2	1	FSM $sinc^{4+1}$	2	1.1E+07	1.1E+07	580	252.63	505.26	248	496

APPENDIX D (On CD)

- D1 0_to_10kg.PNG – A jump change in raw value when loaded with 10kg

APPENDIX E

ADC heat dependency – differences in measurements during different temperatures.

t [°C] ->	Rh 40% 24	10	20	30	40	50	60	70
Tenz(0.0)	8408573	8409171	8408296	8408317	8408957	8409235	8409619	8407933
Tenz(1.1)	8410283	8410603	8409963	8410091	8409280	8408043	8408256	8410070
Tenz(0.1)	8401513	8401428	8401470	8402580	8401705	8402345	8402686	8403219
Tenz(1.0)	8392171	8392320	8392299	8391723	8392341	8392576	8391339	8392427
Tenz(0.0)	8408872	8409896	8408893	8408872	8408296	8408723	8408445	8407166
Tenz(1.1)	8409408	8411115	8401108	8410475	8409515	8408299	8406614	8407744
Tenz(0.1)	8401257	8401278	8409344	8401940	8401513	8400788	8401321	8402260
Tenz(1.0)	8391168	8392555	8392789	8392512	8392128	8392555	8392363	8392661
Tenz(0.0)	8408211	8408403	8407656	8408232	8409597	8406760	8408851	8408424
Tenz(1.1)	8409963	8410134	8400702	8410945	8411777	8405739	8407638	8406102
Tenz(0.1)	8401748	8401812	8409622	8402878	8403241	8400233	8402430	8401065
Tenz(1.0)	8392512	8392448	8392661	8392171	8393365	8390421	8391552	8391531
Tenz(0.0) Mean val.	8408552	8409156,7	8408282	8408474	8408950	8408239	8408972	8407841
Tenz(1.1) Mean val.	8409885	8410617,3	8403924	8410504	8410191	8407360	8407503	8407972
Tenz(0.1) Mean val.	8401506	8401506	8406812	8402466	8402153	8401122	8402146	8402181
Tenz(1.0) Mean val.	8391950	8392441	8392583	8392135	8392611	8391851	8391751	8392206
Tenz(0.0) rozdil 24°-n		-604,66667	875	-192	-476,333	710,667	-732,333	1130,67
Tenz(1.1) rozdil 24°-n		-732,66667	6693	-6579,33	313	2830,33	-142,333	-469,333
Tenz(0.1) rozdil 24°-n		0	-5306	4346	313	1031	-1023,67	-35,6667
Tenz(1.0) rozdil 24°-n		-490,66667	-142	447,667	-476	760,667	99,3333	-455